

An applied mathematical view of meteorological modeling*

Rupert Klein[†]

1 Introduction

The earth's atmosphere is of overwhelming complexity due to a rich interplay between a large number of phenomena interacting on very diverse length and time scales. There are mathematical equation systems which, in principle, provide a comprehensive description of this system. Yet, exact or accurate approximate solutions to these equations covering the full range of complexities they allow for are not available. As a consequence, one of the central themes of theoretical meteorology is the development of simplified model equations that are amenable to analysis and computational approximate solution, while still faithfully representing an important subset of the observed phenomena.

1.1 Governing equations

Throughout this paper we consider the three-dimensional compressible flow equations for an ideal gas with constant specific heat capacities, supplemented with a

*The research presented here has been funded partially by the Deutsche Forschungsgemeinschaft, Grant KL 611/6. Major parts of this work have been achieved in collaboration with Andrew J. Majda (Courant Institute of Mathematical Sciences, New York, NY, USA), Ann Almgren (Lawrence Berkeley Nat. Lab., Berkeley, CA, USA), and Nicola Botta, Antony Owinoh, Susanne Lützenkirchen (Potsdam Institute for Climate Impact Research). The paper has benefitted greatly from elucidating discussions and extensive helpful comments by U. Achatz, M.J. Cullen, J.C.R. Hunt, and V. Petukhov.

[†]FB Mathematik und Informatik, Freie Universität Berlin, Germany, and Potsdam Institut für Klimafolgenforschung (PIK), Potsdam, Germany

number of source terms, as the starting point of our derivations.

$$\begin{aligned}
 \mathbf{v}_t + \mathbf{v} \cdot \nabla \mathbf{v} + \boldsymbol{\Omega} \times \mathbf{v} + \frac{1}{\rho} \nabla p &= \mathbf{S}_v - g\mathbf{k} \\
 p_t + \mathbf{v} \cdot \nabla p + \gamma p \nabla \cdot \mathbf{v} &= S_p \\
 \theta_t + \mathbf{v} \cdot \nabla \theta &= S_\theta,
 \end{aligned} \tag{1}$$

Here \mathbf{v}, p, θ are the fluid flow velocity, the (thermodynamic) pressure, and the fluid's potential temperature. γ is the isentropic exponent, assumed to be constant. $\boldsymbol{\Omega}, g$ are the vector of earth rotation and the acceleration of gravity, \mathbf{k} is a radial unit vector, pointing away from the earth's center. The source terms $\mathbf{S}_u, S_p, S_\theta$ are abbreviations for molecular or turbulent transport terms, for effective energy source terms from radiation, latent heat release from condensation of water vapor, etc..

The potential temperature is a variable, closely related to thermodynamic entropy, and defined by

$$\theta = \frac{p_{\text{ref}}^{\frac{\gamma-1}{\gamma}}}{R} \frac{p^{\frac{1}{\gamma}}}{\rho}, \tag{2}$$

where R is the ideal gas constant. This variable is the answer to the following question: Suppose one isolates an infinitesimally small parcel of air at any location in the atmosphere, and lets the parcel's pressure and density be p, ρ , respectively. What would be the parcel's temperature if it were to undergo an adiabatic and quasi-static, i.e., isentropic, process that leads to a final pressure p_{ref} ?

The equations in (1), (2) account for the vapor-water, water-ice, and vapor-ice phase transitions neither through balance equations for the related species densities, nor through the thermodynamic relations for γ and $\theta(p, \rho)$. While this is certainly an over-simplification for realistic meteorological applications, it allows us to present the key ideas of this work in a transparent fashion. The incorporation of moist processes within the present mathematical framework is work in progress.

Similar comments hold for other effects collected in the effective source terms, $\mathbf{S}_u, S_p, S_\theta$, such as turbulent transport.

1.2 Structure of the rest of the paper

Section 2 will summarize three typical simplified model equation systems that have been developed to describe selected phenomena associated with specific ranges of length and time scales. Models of this type play a central role in meteorology and climate research as they condense the available knowledge regarding the targeted phenomena in a mathematically compact, and computationally tractable fashion.

The derivation of such simplified models generally relies on a combination of judicious physical reasoning and subsequent, sometimes quite intricate, mathematical calculations. The first component, physical reasoning, requires an intimate knowledge of the scientific field, and it is often quite hard to follow for the mathematically trained, but meteorologically untrained. On the other hand, it would be the mathematically trained, who would be in a position to judge, e.g., the well-posedness of the derived reduced model, to show rigorously that solutions of the

model equations are somehow “close” to solutions of the original complex equations, etc.. Thus it is desirable to bridge between the physics-oriented meteorological viewpoint and the mathematical one.

Section 3 addresses this issue by describing a unified mathematical approach to meteorological modelling developed recently by the author, and anticipated in [Klein, 2000]. The approach is based on a set of carefully chosen distinguished limits for several small non-dimensional parameters, and on specializations of a very general multiple-scales asymptotic ansatz.

Section 4 will summarize three instructive applications of the approach, ranging from a re-derivation of the well-known semi-geostrophic theory, [Gill, 1982, Pedlosky, 1987], via one of the recently derived multi-scale models for the tropics, [Majda and Klein, 2003], to numerical methods for (1), (2), that are “well-balanced” with respect to nearly hydrostatic situations. (A numerical method for a complex equation system is called well-balanced w.r.t. some singular limit regime if its accuracy and robustness do not deteriorate as the limit is approached, [Cargo and Roux, 1994].)

Section 5 draws a few conclusions.

2 Phenomena with widely disparate scales

As mentioned in the introduction, atmospheric flows feature a multitude of different length and time scales. While some of these scales are imposed on the air flow externally, e.g., the characteristic lengths of the bottom topography, others are intrinsic to the atmospheric layer on the rotating earth. An intuitive description of these intrinsic scales may be given by reference to the phase speeds of three physically important phenomena, namely

u_{ref}	\sim	10 m/s	Characteristic flow velocity,
c_i	\sim	60 m/s	Typical propagation speed of internal gravity waves,
c_e	\sim	300 m/s	Typical propagation speed of external gravity waves.

The mentioned characteristic length scales are

h_{sc}	\sim	10 km	Pressure scale height: Vertical distance with significant pressure drop.
L_1	\sim	70 km	For flows with horizontal characteristic length L_1 the inertial and Coriolis forces are comparable.
L_i	\sim	500 km	Internal Rossby deformation radius: The distance a typical internal gravity wave with speed c_i would have to travel to be affected by Coriolis effects significantly.
L_e	\sim	3 000 km	Obukhov radius or external deformation radius: Analogous to L_i , but for the much faster barotropic gravity waves with speed c_e . (see “Lamb waves”, [Gill, 1982])
L_p	\sim	20 000 km	The planetary scale.

Some physical arguments for the existence of these scales will be given in section 3 below. The appearance of these separated scales may also be understood, from a mathematical point of view, as being naturally induced by the existence of a single small asymptotic parameter, $\varepsilon \ll 1$, in the sense of multiple scales asymptotics. The section will then “translate” between these two points of view.

Together with the signal speeds u_{ref}, c_i, c_e the length scales just introduced make up an entire grid of different flow regimes as shown in left graph in Figure 1a. Notice, in this context, that

$$t_{ref} \sim \frac{u_{ref}}{h_{sc}} \approx \frac{L_1}{c_i} \approx \frac{L_i}{c_e}. \quad (3)$$

Consider, e.g., the left-most three boxes of the grid in the lowest row, which have the time scale t_{ref} in common. The left-most box represents advection over distances comparable to h_{sc} , the middle box covers the regime of internal gravity waves with the same characteristic frequency, while the right-most box represents the regime of external gravity waves that evolve on this time scale. Similarly, the lowest three boxes of the L_i -column cover, at successively slower time scales, fast external gravity waves, internal gravity waves, and advection over distances comparable to L_i .

Within each of the regimes in the graph, different physical mechanisms dominate, and an associated reduced model equation is conceivable which approximately describes the flow evolution in that regime. Figure 1b shows the regimes to be discussed briefly in this section as examples.

2.1 Climate scale adjustments

Global climate modelling strategies

Even though they are by far not complete, the scale maps in Fig. 1 indicate that the global climate incorporates a very wide range of length and time scales and associated physical processes. Modern climate research proceeds along various pathways

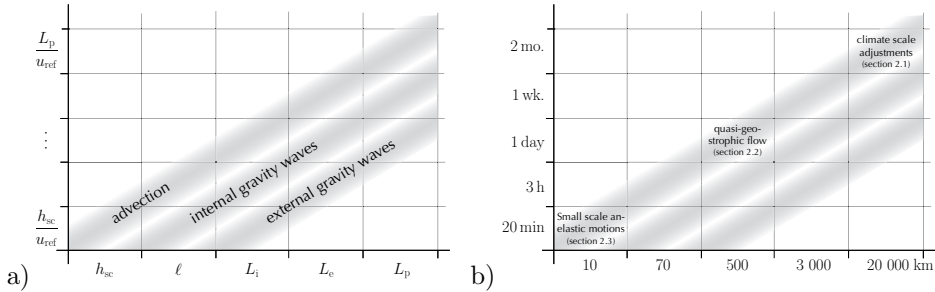


Figure 1. Regimes of length and time scales for flows involving the bulk of the troposphere in the mid-latitudes. The corresponding regimes for near-equatorial and stratosphere flows involve slightly different scales (see, e.g., section 4.2). a) The backbone of a more involved scale diagram that would include the characteristic scales of turbulence, water phase transitions, radiation, boundary layer processes, atmospheric chemistry, etc.. b) Localization of the regimes to be discussed in this section as examples.

in trying to cope with the resulting complexity. One strategy, generally subsumed under the headline of General Circulation Models (GCM), involves the development and numerical solution of a set of model equations that is “as complete as possible”. These avoid model reductions based on pre-assumed dominant length and time scales to the widest possible extent. In practice, one aims at model equations that properly describe *all* scales larger than those one can afford to resolve on the most powerful computers available. Today’s resolutions involve computational grid sizes of about 100 km in the horizontal, 200 m in the vertical direction, and time steps of several minutes. For all processes taking place on smaller length and time scales, and which can therefore not be described explicitly, one introduces “sub-grid scale parameterizations”. These are very similar in spirit to turbulence closures in fluid mechanics, but account for a much larger set of processes, such as small scale (natural) convection due to radiative heating, latent heat release from the condensation of water vapor, interactions of the atmosphere with surface processes near the ground, etc..

Modern GCMs draw their justification and attractiveness from the fact that they directly implement the state-of-the-art knowledge regarding a large number of participating processes. They are “the best climate research can do today” in this sense, and they may be considered as reference and benchmark for alternative modelling approaches. However, the sheer complexity of the simulation data turns their analysis and interpretation into an entire scientific endeavour all by itself, involving sophisticated statistical and combined deterministic / statistical techniques. Moreover, long term, thousands-of-years transients involving interactions of atmosphere, ocean, sea and land ice, terrestrial and oceanic biosphere, land surface processes, etc., are as yet beyond current GCMs’ capabilities. Also, for a range of global climate research questions the small scale, short time details provided by GCM simulations are not only not of interest, but they also shield the view, to some ex-

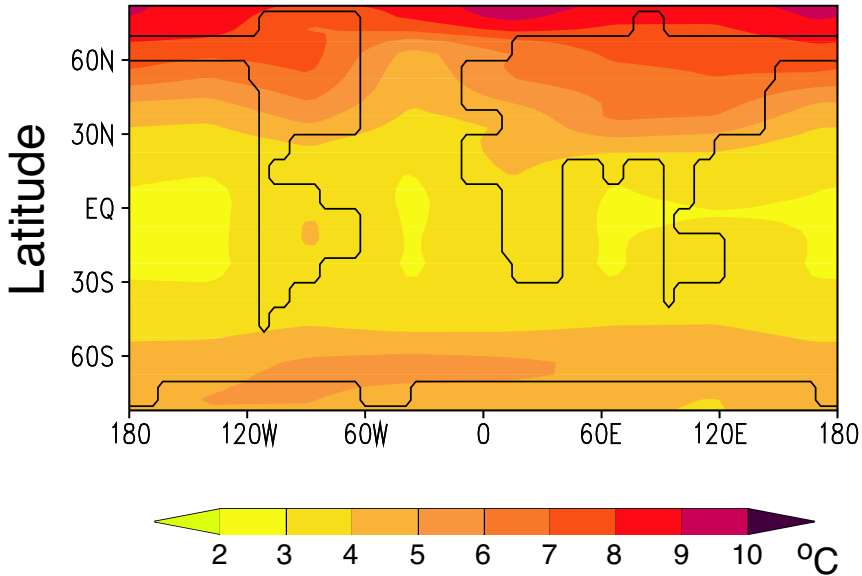


Figure 2. Map of the simulated annual-mean surface air temperature change in the year 2100 for a standard scenario of future CO_2 emissions relative to the year 1800. (Courtesy of Stefan Rahmstorf, Potsdam Institut für Klimafolgenforschung.)

tent, on what are the relevant physical interactions on the very largest scales of the climate system.

More recent developments of “Earth system Models of Intermediate Complexity” (EMIC) address these issues, [Saltzman, 1978, Petoukhov et al., 2000, Stone and Yao, 1990]. These models are designed to describe *only* these largest scales and to consider everything below, say, the external Rossby deformation radius L_e as “small scale processes” to be parameterized, see, e.g., [Stone and Yao, 1990]. In comparison with full-fledged GCMs, such EMICs have the advantage of very high computational efficiency and, by representing only the “climate scales”, they provide the desired direct view of the large scale mean variables. Figure 2 shows, as an example, the computed deviations of the large scale, long time temperature mean values between the year 1800 and the year 2100 as obtained with the CLIMBER-2 EMIC by Rahmstorf and Ganopolski [1999]. The figure clearly reveals that the simulations do not display any spacial variations comparable to the typical cyclonic / anti-cyclonic patterns seen on daily weather charts (see section 2.2 below). In fact, such variability is parameterized within the CLIMBER-2 model by averaging over an assumed Gaussian statistics for these modes.

Structure of an intermediate complexity atmosphere model

Here we report briefly on the structure of POTSDAM-2 (POTsdam Statistical Dynamical Atmosphere Model), the atmosphere component of the CLIMBER-2 EMIC, as described by Petoukhov et al. [2000].

There are only two two-dimensional unsteady evolution equations

$$\frac{\partial Q_T}{\partial t} = \nabla_{\parallel} \cdot \mathbf{F}_T + S_T \quad (4)$$

$$\frac{\partial Q_q}{\partial t} = \nabla_{\parallel} \cdot \mathbf{F}_q + S_q \quad (5)$$

for the depth-averaged thermal energy, Q_t , and water content, Q_q , which are defined as

$$Q_T = \int_{z_s}^{H_a} \rho T dz \quad \text{and} \quad Q_q = \int_{z_s}^{H_a} \rho q dz, \quad (6)$$

respectively. Here T, q, ρ are temperature, water vapor mass fraction, and air density, and z_s, H_a are the vertical levels of the bottom topography and of the top of the atmosphere. ∇_{\parallel} denotes the horizontal gradient operator. The flux \mathbf{F}_T is given by

$$\mathbf{F}_T = \int_{z_s}^{H_a} \rho \left(\mathbf{u}\theta + \widehat{\mathbf{u}'\theta'} + \mathbf{D}^{\theta} \right) dz. \quad (7)$$

This expression includes advection of potential temperature by the large scale wind field, \mathbf{u} , the effective transport of potential temperature by synoptic scale fluctuations, \mathbf{u}', θ' , and the transport by turbulent motions on even smaller scales subsumed in \mathbf{D}^{θ} . (The humidity flux \mathbf{F}_q has a similar representation).

These equations determine the evolution of the surface fields

$$T_s(t, \mathbf{x}), \quad q_s(t, \mathbf{x})$$

of temperature and humidity. Closed expressions for the various integrals are obtained by assuming piecewise linear and exponential vertical structures for T, θ, q, ρ , respectively, namely

$$T = \begin{cases} T_s(t, \mathbf{x}) + \Gamma(z - z_s) & \text{for } z_s \leq z < H_t \\ T_s(t, \mathbf{x}) + \Gamma(H_t - z_s) & \text{for } H_t \leq z < H_a \end{cases} \quad (8)$$

$$\theta = T_s(t, \mathbf{x}) - \Gamma_a(z - z_s), \quad (9)$$

$$q = q_s(t, \mathbf{x}) \exp\left(-\frac{z - z_s}{H_e}\right), \quad (10)$$

$$\rho = \rho_* \exp\left(-\frac{z}{h_{sc}}\right). \quad (11)$$

Here ρ_* , h_{sc} , H_e are constants, and the coefficients Γ , Γ_a , H_t are related to T_s , q_s via explicit algebraic functions.

The large scale horizontal wind field is composed of geostrophic and ageostrophic components (see section 2.2), so that

$$\mathbf{u} = \mathbf{u}_g + \mathbf{u}_a, \quad (12)$$

where \mathbf{u}_g is determined by the current temperature field T and the sea level pressure p_0 via

$$f\mathbf{k} \times \mathbf{u}_g = -\frac{1}{\rho_*}\nabla p_0 - g\nabla \int_0^z \frac{T}{T_*} dz' \quad (13)$$

with T_* another constant, and f the vertical component of the earth rotation vector $\boldsymbol{\Omega}$. The ageostrophic field \mathbf{u}_a is proportional to the gradient of the sea level pressure p_0 . Finally, the sea level pressure is expressed in terms of the temperature distribution $T(t, \mathbf{x}, z)$, using semi-empirical relations for the zonally averaged motions. The reader is referred to [Petoukhov et al., 2000] for details.

While the relations just described for the large scale wind field can be derived analytically within a rational scaling (asymptotic) analysis, the expressions given by Petoukhov et al. [2000] for the turbulent and macro-turbulent fluxes \mathbf{D}^θ , $\widehat{\mathbf{u}'\theta'}$, and for the source terms S_T , S_q in (4) and (5) are semi-empirical closures similar to turbulence closures in fluid mechanics.

For future reference, we summarize the mathematical structure of the large scale, long time evolution equations for the atmosphere: The two-dimensional fields, $T_s(t, \mathbf{x})$, $q_s(t, \mathbf{x})$, which represent the surface values of temperature and humidity, are advanced in time by solving depth-averaged balance equations for internal energy and water content. These balance equations involve horizontal fluxes due to large scale advection, and macro- and smaller scale turbulence, as well as other source terms related to radiation, evapo-transpiration, precipitation, etc.. The large scale wind field is related algebraically to gradients of the primary fields T_s , q_s as a result of a scale or asymptotic analysis which pre-assumes the characteristic length and time scales of interest. For the various source terms and turbulence effects, semi-empirical parameterizations are introduced that ultimately lead to a closed equation set for the unknown fields $T_s(t, \mathbf{x})$, $q_s(t, \mathbf{x})$.

Notes on the closure schemes for fast processes

EMICs are often criticized for over-simplified representations of possibly crucial small scale processes, and there are a number of research activities on the way that aim at (i) an overall model design that still addresses only the large scale, long time climate variables, but which (ii) incorporates more sophisticated closure schemes for the non-resolved processes. For example Conaty et al. [2001] include unsteady evolution equations for the ensemble characteristics of smaller scales instead of the static relations mentioned above. Achatz and Branstator [1999] combine a fluid dynamics model for the large scale motions with a closure scheme that directly incorporates the statistics generated by GCM simulations. Their model captures

the energetically most important large scale patterns with considerable accuracy and it provides insight into atmospheric variability on time scales that are normally not accessible with statistical dynamical models as described above. This fosters hope that more sophisticated, explicitly time dependent closure schemes might make a much wider range of applications amenable to intermediate complexity models without having to accept the full complexity of a general circulation model.

In this context, a novel approach to obtaining effective *stochastic* equations for the large scale, long time variables has recently been proposed by A.J. Majda et al. [Majda et al., 2003]. It is assumed, to start with, that a decomposition of the original complex dynamics into equations for the slow and for the fast modes, respectively has been established. The approach then consists of two steps: First, a carefully chosen *stochastic* closure is introduced in the equations for the fast variables so as to make them tractable by the tool kit of stochastic differential equations. No approximations are made at that stage in the equations for the slow modes. Secondly, appropriate stochastic closures for the “slow equations” are *derived systematically* by stochastic projection procedures. The resulting effective closure schemes have rich mathematical structures that are hard to anticipate in an approach that tries to directly guess the functional form of such terms without this two-step procedure.

The next subsection considers in more detail the dynamics on the next smaller “synoptic scales”, which appears in low-resolution models and EMICs only through such effective closure schemes.

2.2 Synoptic Scales

Scalings considerations

Figure 3 shows one of the typical results of the “synoptic analysis” of global atmospheric flow simulations. The contours indicate the “geopotential height” $H = \Phi/g_c$ of a surface of constant pressure $p = 500$ hPa. Here Φ is the effective geopotential, which is the sum of the earth’s gravitational potential and the potential associated with the centripetal forces due to the earth’s rotation, and g_c is a constant reference value of the gravitational acceleration which varies by about 0.3% over the globe, [Gill, 1982]. Countour labels show H measured in units of 10 m. The geopotential height approximates the height of a pressure surface above sea level up to deviations of the order of one percent.

The Figure exhibits a collection of “synoptic eddies” of high and low pressure around which the main air flow circulates as indicated. The characteristic diameter of these structures is about 500 . . . 1 000 km, i.e., comparable to the internal Rossby deformation radius, L_i , and their characteristic evolution time scale is about 1 . . . 5 days. Fig. 1b locates the evolution of these structures in the regime diagram. Assuming a flow field with such characteristic length and time scales, the important “quasi-geostrophic model” is derived, e.g., in [Pedlosky, 1987], as the leading order approximation in terms of the Rossby number based on the internal deformation radius L_i ,

$$\text{Ro}_{L_i} = \frac{u_{\text{ref}}}{\Omega L_i} \ll 1. \quad (14)$$

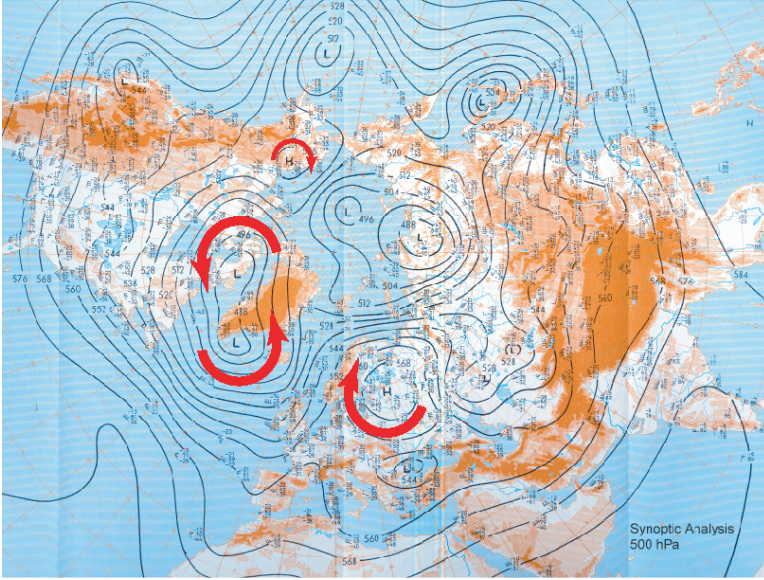


Figure 3. A typical contour plot of the geopotential height of the 500 hPa surface over a large part of the northern hemisphere. (Courtesy of Peter Névir, Institut für Meteorologie, Freie Universität Berlin)

An asymptotic expansion for the solution vector \mathbf{U} for this regime would read

$$\mathbf{U} = \sum_i \text{Ro}_{L_i}^i \mathbf{U}^{(i)}(T, \mathbf{X}, Z) \quad (15)$$

where

$$T = \frac{tu_{\text{ref}}}{L_i}, \quad \mathbf{X} = (X, Y) = \frac{\mathbf{x}}{L_i}, \quad Z = \frac{z}{h_{\text{sc}}} \quad (16)$$

are non-dimensional time, and horizontal and vertical space coordinates. A detailed derivation is given, e.g., in [Pedlosky, 1987].

The quasi-geostrophic model

The resulting quasi-geostrophic equations are formulated in the β -plane approximation, i.e., they describe the flow of a shallow layer of fluid over a rotating plane with spatially varying Coriolis coefficient

$$f = f_0 + \beta Y. \quad (17)$$

Here $f = \boldsymbol{\Omega} \cdot \mathbf{k}$ is the projection of the earth rotation vector onto the vertical unit vector \mathbf{k} in a tangent plane to the earth's surface, f_0 is its value at the location of contact of the plane with the earth's geometry, and β is its variation with distance in the northern direction measured by the cartesian coordinate Y .

The vertical momentum balance reveals that the pressure field is hydrostatic to several orders in terms of the expansion parameter. In particular, there are time independent leading order hydrostatic pressure and density distributions $p_0(z), \rho_0(z)$, and a background stratification of potential temperature characterized by second order deviations, $\Theta_2(z)$, from a constant reference value. The first perturbation pressure with non-trivial horizontal variation, $p' = \rho_0(z)\pi$, still satisfies a hydrostatic relation

$$\frac{\partial \pi}{\partial z} = \theta', \quad (18)$$

where θ' denotes the third order perturbation of potential temperature.

Gradients of the perturbation pressure balance the Coriolis forces at leading order in the horizontal direction, so that

$$f_0 \mathbf{k} \times \mathbf{u} = -\nabla_{\mathbf{X}} \pi. \quad (19)$$

Here \mathbf{u} is the horizontal flow velocity component. This equation is insufficient to determine a flow field *including* its temporal evolution. As usual in singular perturbation analyses, the missing evolution equation is obtained through a consistency condition at the next order. The result is a transport equation for the ‘‘potential vorticity’’, q ,

$$\left(\frac{\partial}{\partial T} + \mathbf{u} \cdot \nabla_{\mathbf{X}} \right) q = 0, \quad (20)$$

where

$$q = \zeta + \beta Y + \frac{f_0}{\rho_0} \frac{\partial}{\partial Z} \left(\frac{\rho_0 \theta'}{d\Theta_2/dZ} \right) \quad (21)$$

and

$$\zeta = \frac{1}{f_0} \nabla^2 \pi \quad (22)$$

is the vorticity associated with the horizontal velocity field \mathbf{u} . This is the appropriate specialization to quasi-steady flow of a thin fluid layer on a rotating plane of Ertel’s general conservation law for potential vorticity, see [Schröder, 1997]. Now (18)–(22) form a closed set of equations for $\zeta, \pi, \theta, \mathbf{u}$.

The physical meaning of the transport equation (20) is readily understood considering that it is equivalent to the transport equation for vertical vorticity

$$\zeta_T + \mathbf{u} \cdot \nabla_{\mathbf{X}} \zeta + \beta v + f_0 \nabla_{\mathbf{X}} \cdot \mathbf{u}' = 0, \quad (23)$$

where v is the horizontal flow velocity in the direction of the Y -coordinate, and \mathbf{u}' is the first order horizontal flow velocity perturbation. The potential vorticity conservation law (20) is obtained from (23) using the identity $v \equiv (\partial_T + \mathbf{u} \cdot \nabla_{\mathbf{X}}) Y$, and by eliminating $\nabla_{\mathbf{X}} \cdot \mathbf{u}'$ using mass conservation, $\rho_0 \nabla_{\mathbf{X}} \cdot \mathbf{u}' + (\rho_0 w')_Z = 0$, and the transport equation for potential temperature (entropy) $(\partial_T + \mathbf{u} \cdot \nabla_{\mathbf{X}}) \theta + w' \frac{d\Theta_2}{dZ} = 0$.

Equation (23) shows that, as the vorticity ζ is advected horizontally, it is augmented by variations of the vertical component of the earth rotation vector, and affected by vortex stretching. These are, in fact, the essential effects determining

the evolution of the “synoptic eddies” seen in Fig. 3. Notice that the present discussion, which closely follows Pedlosky’s classical textbook presentation, [Pedlosky, 1987], does not include source terms from radiative balance, latent heat conversion, boundary layer effects, etc., so that it reveals only the fluid dynamical aspects of these synoptic scale flows.

2.3 Small scale anelastic flows

Here we consider motions on scales comparable to or smaller than the pressure scale height $h_{sc} \sim 10$ km, and on the associated advection time scale of $t_{ref} = h_{sc}/u_{ref} \sim 20$ min. In this flow regime, one of the prominent issues is the removal of inessential acoustic modes in a reduced model.

The full compressible flow equations from (1) feature various flow modes, including “high frequency” acoustic waves. Here “high frequency” denotes acoustic modes with characteristic frequencies higher than 1 min^{-1} . A plausibility argument states that sizeable elastic perturbations cannot establish in the atmosphere, because acoustic waves rapidly redistribute the associated energy and lead to an equilibration void of any acoustic modes. This intuitive explanation has been quantified through asymptotic analysis for vanishing Mach number in non-rotating flows without gravity (see, e.g., [Schneider, 1978, Majda and Sethian, 1985]) and backed up by rigorous justifications, e.g., in [Ebin, 1982, Klainerman and Majda, 1982, Schochet, 1994].

In the absence of energy source terms, such an analysis results in the classical variable density, incompressible flow equations, with zero velocity divergence.

Three-dimensional motions

However, if one includes the effects of gravity and energy source terms from radiation or latent heat conversion, and allows for vertical motions comparable in scale to the pressure scale height, then two distinctly different flow regimes can be identified, [Ogura and Phillips, 1962, Durran, 1989, Klein, 2000]. The first regime involves nearly neutral stratification of the atmosphere, so that parcels of air can move freely in the vertical direction without being constrained by buoyancy effects. In this situation, discussed first by Ogura and Phillips, [Ogura and Phillips, 1962], the flow is governed by the anelastic equations in the Boussinesq approximation, so that

$$\begin{aligned}
 \mathbf{u}_t + \mathbf{u} \cdot \nabla \mathbf{u} + w \mathbf{u}_z + \frac{1}{\rho_0} \nabla p' &= \mathbf{S}_u \\
 w_t + \mathbf{u} \cdot \nabla w + w w_z + \frac{1}{\rho_0} p'_z &= \theta' + S_w \\
 \theta'_t + \mathbf{u} \cdot \nabla \theta' + w \theta'_z &= S_{\theta'} \\
 \nabla \cdot (\rho_0 \mathbf{u}) + \partial_z (\rho_0 w) &= 0
 \end{aligned} \tag{24}$$

where $\rho_0(z)$ is a time independent, horizontally homogeneous density stratification. Given suitable functional expressions for the source terms $\mathbf{S}_u, S_w, S_{\theta'}$, these equa-

tions govern the temporal evolution of the horizontal and vertical velocity components \mathbf{u}, w , and the potential temperature perturbation θ' . The perturbation pressure p' is determined, as in the classical case of incompressible flows, by a Poisson-type equation obtained by analyzing the consequences of the divergence constraint (24)₄ for the two momentum equations (24)_{1,2}. The complexity and structure of these equations is comparable to that of the classical three-dimensional incompressible flow equations. They are particularly useful in studies of the atmospheric boundary layer, where the assumption of nearly neutral stratification is well justified. (See [Durran, 1989] for an interesting generalization of (24), and the discussions in [Botta et al., 1999, Klein, 2000].)

Quasi two-dimensional weak temperature gradient flows

In their original derivation Ogura and Phillips [1962] explicitly state that the stratification of potential temperature in the atmosphere must be nearly neutral to arrive at the reduced equation system from (24). Zeytounian [1991] pursues an analogous scaling analysis but relaxes that constraint. The result is a system of equations in which the vertical velocity is entirely dominated by buoyancy. In the absence of energy source terms he find that all parcels of air are forced to reside within their respective vertical levels of neutral buoyancy, so that vertical motions are suppressed. This holds at least if the shortest relevant time scale is that of advective motions. Internal gravity waves on shorter time scales *will* induce vertical displacements, but their description would require a multiple time scale analysis, see, e.g., [Embid and Majda, 1998, Babin et al., 2002] and section 3 below.

Klein [2000] compares both the near-neutral and the buoyancy-controlled regimes and includes energy source terms. For the buoyancy-controlled regime, the following system of equations obtains,

$$\begin{aligned} \mathbf{u}_t + \mathbf{u} \cdot \nabla \mathbf{u} + w \mathbf{u}_z + \frac{1}{\rho_0} \nabla p' &= \mathbf{S}_u \\ w &= \frac{S_\theta}{d\Theta_2/dz} \\ \nabla \cdot (\rho_0 \mathbf{u}) + \partial_z(\rho_0 w) &= 0. \end{aligned} \tag{25}$$

Here \mathbf{u}, w, p' are the horizontal and vertical flow velocities and the perturbation pressure as before, while $\Theta_2(z)$ is the background stratification of potential temperature responsible for the deviations from the Ogura and Phillips' regime. These equations are, as far as fluid dynamics is concerned, essentially two-dimensional, whereas the vertical velocity appears as an algebraically determined auxiliary quantity. Similar equation sets have been derived in other contexts including, in particular, near-equatorial motions at much larger horizontal scales, in [Charney, 1963, Held and Hoskins, 1985, Browning et al., 2000].

While (25) has been derived by [Klein, 2000] via low Mach number asymptotics, there is an alternative derivation that is based on the a priori assumption that horizontal gradients of temperature often very weak in practical applications. Referring to this line of thought, models of this class have been labelled "Weak

Temperature Gradient” approximations in recent studies of near-equatorial flows, [Neelin, 2000, A. Sobel et al., 2001, Bretherton and Sobel, 2001, Majda and Klein, 2003].

The reader may wonder, how any reasonable bottom boundary condition, such as $w \equiv 0$ at $z = 0$ could be maintained under (25), unless the energy source term represented by S_θ would be unnaturally constrained. The asymptotic limit considered here has obviously removed one degree of freedom in posing boundary conditions that had been present in the original three-dimensional flow equations from (1). This is a typical case of a singular limit in which the mathematical type of the equation changes when the limit is approached. In the present case, the failure of solutions of (25) to comply with the physically relevant bottom boundary conditions is a hint that a comprehensive analysis will have to include a near-bottom boundary layer, in which different length and/or time scalings have to be assumed. Asymptotic matching of the boundary layer solution to the bulk flow WTG equations will likely lead to the desired physically consistent asymptotic representation all the way down to the bottom of the atmospheric layer.

In the presence of non-trivial orography or surface conditions the near-bottom flow can induce highly non-trivial effects. In this case appropriate boundary layer theories need to be developed, [Hunt et al., 1988, Newley et al., 1991], and their coupling to the bulk of the troposphere in the sense of asymptotic matching needs to be addressed.

2.4 Looking back

Looking back, we have seen in this section that the mathematical structure of reduced models for atmospheric motions depends heavily on the considered length and time scales, and on particular assumptions regarding specifics of the considered flow regime.

In the next section we introduce a unified approach to the analysis of such diverse scaling regimes that lets us get away with a minimal set of a priori assumptions. The approach provides a systematic basis for structuring further mathematical analyses and discussions. Furthermore, it incorporates multiple scales asymptotic ideas by design, thereby providing a natural framework for studying interactions between such different phenomena as seen in this section.

3 A Unified Mathematical Modelling Approach

3.1 Overview

The derivation of simplified model equations of theoretical meteorology generally relies on a combination of judicious physical reasoning and subsequent, often intricate, mathematical calculations. The first component, physical reasoning, requires an intimate knowledge of the scientific field, and it is often hard to follow for the mathematically trained, but meteorologically untrained. Readers belonging to this group might benefit from the unified mathematical approach proposed in this paper, which reveals some common underlying structures of meteorological scaling

theories. Meteorologists may appreciate the potential of the present approach for systematically addressing multiple scales problems, and for structuring mathematical discussions regarding model derivations and the construction of appropriate numerical techniques.

The approach is based on a set of carefully chosen distinguished limits for several small non-dimensional parameters, and on specializations of a very general multiple-scales asymptotic *ansatz*. Here is a summary of the key ideas, an early version of which appeared in [Klein, 2000]:

1. *Scale-independent reference quantities*

First we collect a set of physical quantities that have well-defined characteristic values in the majority of atmosphere flow applications *independently* of the characteristic length and time scales of any particular phenomena.

2. *Universal non-dimensional parameters*

Next we combine these characteristic values to form non-dimensional parameters, say π_1, π_2, π_3 . These parameters will have more or less universally accepted typical values.

3. *Distinguished limits*

We then group these parameters in a carefully chosen distinguished limit

$$\begin{aligned} \pi_1 &= \pi_1^*, \\ \pi_2 &= \varepsilon^2 \pi_2^*, \quad \text{where} \quad \pi_j^* = O_s(1) \quad \text{as} \quad \varepsilon \rightarrow 0 \quad \text{for} \quad j \in \{1, 2, 3\}. \\ \pi_3 &= \varepsilon^3 \pi_3^*, \end{aligned}$$

Here we have used the notation $f = O_s(\varepsilon)$ as $\varepsilon \rightarrow 0$ iff $0 < \limsup_{\varepsilon \rightarrow 0} \|f\| < \infty$. Subsequently we employ $\varepsilon \ll 1$ as an asymptotic expansion parameter. This step defines a single asymptotic regime for the scale-independent dimensionless parameters π_1, π_2, π_3 which most atmospheric flows belong to.

4. *Dimensionless governing equations*

Using only the scale-independent reference quantities from the first step, we non-dimensionalize the governing equations. Because these reference quantities are related via the distinguished limits from the previous step, the resulting system of dimensionless equations includes the constants π_i^* and the small parameter ε as the only dimensionless characteristic numbers.

5. *Multiple-scales asymptotic expansions*

By definition, reduced model equations of theoretical meteorology obtained through *scale analysis* describe phenomena that are characterized by some typical length and time scales and fluctuation amplitudes. Here we account for such scalings through a general multiple scales asymptotic *ansatz* in terms of ε . The solution $\mathbf{U}(t, \mathbf{x}, z; \varepsilon)$ of the multi-dimensional compressible flow equations is expressed as

$$\mathbf{U}(t, \mathbf{x}, z; \varepsilon) = \sum_{i \in \mathbb{N}} \phi^{(i)}(\varepsilon) \mathbf{U}^{(i)}\left(\frac{t}{\varepsilon}, t, \varepsilon t, \varepsilon^2 t, \dots, \frac{\mathbf{x}}{\varepsilon}, \mathbf{x}, \varepsilon \mathbf{x}, \varepsilon^2 \mathbf{x}, \dots, \frac{z}{\varepsilon}, z\right), \quad (26)$$

where the $\phi^{(i)}$ form an asymptotic sequence, such as $\phi^{(i)}(\varepsilon) = \varepsilon^i$, and (t, \mathbf{x}, z) are time, horizontal space, and vertical coordinates, respectively. More complex asymptotic sequences and non-powerlaw scalings of the coordinates are to be adopted where necessary. See, e.g., [Hunt et al., 1988, Newley et al., 1991] for examples necessitating non-powerlaw expansions.

Specializations of this formulation, obtained by reducing the set of coordinates to merely one time, one horizontal, and one vertical coordinate, have allowed us to recover systematically a large collection of well-known reduced models by applying techniques of formal single-scale asymptotic analysis. Table 1 displays a list of examples (in which t, \mathbf{x}, z have been non-dimensionalized with $t_{\text{ref}} = \ell_{\text{ref}}/u_{\text{ref}}$, $\ell_{\text{ref}} \sim 10$ km, $u_{\text{ref}} \sim 10$ m/s; see Tables 2, 3 and equations (29)–(31)). Notice that throughout this list the parameter ε has exactly the same meaning as established under item 3 above. Thus, even though we address a multitude of different regimes *in terms of length and time scales*, the fundamental distinguished limit for the dimensionless scale-independent parameters π_1, π_2, π_3 remains the same.

Table 1. *Coordinate scalings and associated classical models.*

Coordinates	Resulting model describes ...
$\mathbf{U}^{(i)}\left(\frac{t}{\varepsilon}, \mathbf{x}, \frac{z}{\varepsilon}\right)$	Linear small scale internal gravity waves
$\mathbf{U}^{(i)}(t, \mathbf{x}, z)$	Anelastic & pseudo-incompressible flows
$\mathbf{U}^{(i)}(\varepsilon t, \varepsilon^2 \mathbf{x}, z)$	Gravity waves influenced by Coriolis effects
$\mathbf{U}^{(i)}(\varepsilon^2 t, \varepsilon^2 \mathbf{x}, z)$	Mid-latitude quasi-geostrophic “QG” flow
$\mathbf{U}^{(i)}(\varepsilon^2 t, \varepsilon^2 \mathbf{x}, z)$	Equatorial weak temperature gradient flow
$\mathbf{U}^{(i)}\left(\varepsilon^2 t, \frac{1}{\varepsilon} \xi(\varepsilon^2 \mathbf{x}), z\right)$	Semi-geostrophic flow
$\mathbf{U}^{(i)}\left(\varepsilon^{\frac{3}{2}} t, \varepsilon^{\frac{5}{2}} \mathbf{x}, \varepsilon^{\frac{5}{2}} y, z\right)$	Tropical Kelvin, Yanai, and Rossby Waves

The general multiple scales *ansatz* from (26) enables us to further study interactions between phenomena acting on separate scales. For example, according to Table 1 we could consider an expansion based on the coordinate set $(\varepsilon t, \varepsilon^2 t, \varepsilon^2 \mathbf{x}, z)$ to analyze the interaction of long-wavelength gravity waves that are influenced by Coriolis effects with balanced geostrophic motions. (See section 4.2 for an example involving multiple scales in the tropics.)

3.2 Asymptotic characterization of atmosphere flows

Scale-independent reference quantities

There are a few physical quantities that have quite robustly agreed-upon typical values under a wide range of atmospheric flow conditions and independently of the particular length and time scales that might otherwise characterize the situation. Table 2 collects quantities related to the rotating earth, table 3 lists typical reference values for the main fluid dynamical variables, i.e., the thermodynamic pressure and air density near the earth's surface, and a characteristic flow velocity. While there are phenomena where flow velocities exceed the listed 10 m/s considerably, as in high-altitude jet streams and severe storms, the majority of the flow phenomena of interest in meteorology are well characterized by flow velocities of several meters per second.

Table 2. *Properties of the rotating earth*

Earth's radius	a	\sim	$6 \cdot 10^6$	m
rotation frequency	Ω	\sim	10^{-4}	s^{-1}
acceleration of gravity	g	\sim	10	m/s^2

Table 3. *Aerothermodynamic conditions*

thermodynamic pressure	p_{ref}	\sim	10^5	kg/ms^2
air flow velocity	u_{ref}	\sim	10	m/s
air density	ρ_{ref}	\sim	1	kg/m^3

Universal non-dimensional parameters

With mass, length, and time these six quantities involve three fundamental physical dimensions, so that Buckingham's theorem, [Buckingham, 1915], allows us to form three independent dimensionless parameters. Let

$$c_{\text{ref}} = \sqrt{\frac{p_{\text{ref}}}{\rho_{\text{ref}}}} \sim 300 \text{ m/s},$$

denote the speed of long wavelength (barotropic) gravity waves in the atmosphere, which is proportional to the speed of sound at reference conditions. Then the following dimensionless combinations turn out to be convenient for the subsequent developments:

$$\begin{aligned}
\pi_1 &= \frac{c_{\text{ref}}}{\Omega a} \sim 0.5 \sim 1, \\
\pi_2 &= \frac{u_{\text{ref}}}{c_{\text{ref}}} \sim 3 \cdot 10^{-2} \ll 1, \\
\pi_3 &= \frac{\Omega c_{\text{ref}}}{g} \sim 3 \cdot 10^{-3} \ll 1.
\end{aligned} \tag{27}$$

(We discuss the relation of these parameters to more familiar ones, such as the Rossby, Mach, and Froude numbers, in section 3.3 below.)

These order-of-magnitude estimates are appropriate for a majority of atmospheric flow phenomena, no matter what are their characteristic length and time scales. In constructing a generalized formal approach to atmosphere modelling we are therefore interested in regimes that are compatible with these scalings.

Distinguished limits

When faced with multiple asymptotically small parameters, an important issue is the precise path along which the parameters are to approach their respective limiting values. Consider, e.g., Fig. 4 which displays the space spanned by two parameters ϵ and δ supposed to characterize some physical system. In an actual application these parameters are “small” in analogy with $u_{\text{ref}}/c_{\text{ref}}$ and $\Omega c_{\text{ref}}/g$ in (27). Thus we may wish to analyze the system under a limit process that sends $\epsilon \rightarrow 0$ and $\delta \rightarrow 0$. If the system is nonlinear the result of the analysis will depend on the path in the ϵ - δ -plane. Possible paths are the sequential limits I or II (see the figure) or any “distinguished limit” such as III, where $\delta = \hat{\delta}(\epsilon) = o(1)$ as $\epsilon \rightarrow 0$, and $\hat{\delta}(\cdot)$ is an appropriate scaling function. Because of the path-dependence of the resulting asymptotic limit equations, the choice of an appropriate distinguished limit is crucial.

Notice also that distinguished asymptotic limits exist under much weaker conditions than multiple parameter expansions that consider each of the small parameters as independent. A multiple parameter expansion in effect seeks to determine the first and higher Fréchet derivatives of solutions of the considered equations with respect to the set of parameters, whereas a distinguished limit corresponds to a particular version of a directional or Gateaux derivative. For functions of multiple variables it is known that only if all Gateaux derivatives are continuous does the Fréchet derivative exist! In this sense, the concept of a distinguished asymptotic limit is more general than that of a multiple parameter asymptotic expansion.

One of the somewhat surprising conclusions of the present work is that a large collection of simplified models of theoretical meteorology obtains with *one and the same* distinguished limit amongst the non-dimensional parameters from (27), namely

$$\pi_1 = \frac{c_{\text{ref}}}{\Omega a} = \pi_1^*, \quad \pi_2 = \frac{u_{\text{ref}}}{c_{\text{ref}}} = \varepsilon^2, \quad \pi_3 = \frac{\Omega c_{\text{ref}}}{g} = \varepsilon^3 \pi_3^*, \quad \text{as } \varepsilon \rightarrow 0. \tag{28}$$

Here π_1^*, π_3^* are independent of ε , which we now adopt as the expansion parameter

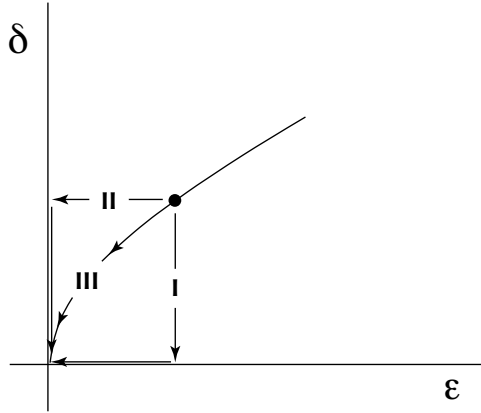


Figure 4. *Limit processes in an asymptotic system with two small parameters*

in subsequent formal asymptotic analyses. (By the way, the specific values shown in (27) suggest a range of values $\varepsilon^{-1} \sim 2\pi \dots 7$ in practice.)

Dimensionless governing equations

The aerothermodynamic characteristic values from Table 3 and the ideal gas constant R from (2) now serve as reference quantities for non-dimensionalization. The resulting dimensionless variables read

$$\hat{p} = \frac{p}{p_{\text{ref}}}, \quad \hat{\mathbf{v}} = \frac{\mathbf{v}}{u_{\text{ref}}}, \quad \hat{\rho} = \frac{\rho}{\rho_{\text{ref}}}, \quad \hat{\theta} = \frac{\theta}{T_{\text{ref}}}, \quad (29)$$

where $T_{\text{ref}} = p_{\text{ref}}/(R\rho_{\text{ref}})$. Using in addition the acceleration of gravity g , we define reference length and time scales as

$$h_{\text{sc}} = \frac{p_{\text{ref}}}{g\rho_{\text{ref}}}, \quad t_{\text{ref}} = \frac{h_{\text{sc}}}{u_{\text{ref}}}, \quad (30)$$

and dimensionless space and time coordinates

$$\hat{t} = \frac{t}{t_{\text{ref}}}, \quad \hat{\mathbf{x}} = \frac{\mathbf{x}}{h_{\text{sc}}}, \quad \hat{z} = \frac{z}{h_{\text{sc}}}. \quad (31)$$

Dropping the “hat”-indicator for dimensionless variable for convenience again, we obtain the dimensionless governing equations

$$\begin{aligned} \mathbf{v}_t + \mathbf{v} \cdot \nabla \mathbf{v} + \varepsilon \pi_3^* \boldsymbol{\Omega} \times \mathbf{v} + \frac{1}{\varepsilon^4} \frac{1}{\rho} \nabla p &= \mathbf{S}_v - \frac{1}{\varepsilon^4} \mathbf{k}, \\ p_t + \mathbf{v} \cdot \nabla p + \gamma p \nabla \cdot \mathbf{v} &= S_p, \\ \theta_t + \mathbf{v} \cdot \nabla \theta &= S_\theta. \end{aligned} \quad (32)$$

Notice that these equations are still *equivalent* to the original dimensional equations from (1), since we have merely chosen a particular set of units of measurement.

Multiple scales and related asymptotic expansions

Atmospheric flow phenomena are characterized by a multitude of different length and time scales and by varying typical amplitudes of the variables $\mathbf{U} = (p, \theta, \mathbf{v}, \rho)$. We capture this variability through the general multiple scales asymptotic *ansatz*

$$\mathbf{U}(t, \mathbf{x}, z; \varepsilon) = \sum_{i \in \mathbb{N}} \phi^{(i)}(\varepsilon) \mathbf{U}^{(i)}\left(\frac{t}{\varepsilon}, t, \varepsilon t, \varepsilon^2 t, \dots, \frac{\mathbf{x}}{\varepsilon}, \mathbf{x}, \varepsilon \mathbf{x}, \varepsilon^2 \mathbf{x}, \dots, \frac{z}{\varepsilon}, z\right). \quad (33)$$

Here the $\phi^{(i)}$ are asymptotic scaling functions satisfying

$$\phi^{(i+1)}(\varepsilon) = o(\phi^{(i)}(\varepsilon)) \quad \text{as} \quad \varepsilon \rightarrow 0. \quad (34)$$

In this paper we will consider cases where $\phi^{(i)}(\varepsilon) = \varepsilon^i$ and/or $\phi^{(i)}(\varepsilon) = \varepsilon^{i+\frac{1}{2}}$. More general asymptotic sequences as well as more general coordinate scalings may also arise, [Hunt et al., 1988, Newley et al., 1991].

Specializations of the tuple of arguments in (33) as given in Table 1 involving one coordinate each for time, and for the horizontal and vertical directions, respectively, induce standard single-scale asymptotic expansions. They allow us to re-derive a considerable collection of well-known reduced models of theoretical meteorology, and this may be considered as a “validation” of the present approach. If we retain more than one coordinate for either of the independent variables, as in $\mathbf{U}^{(i)}(t, \varepsilon t, \mathbf{x}, z)$, multiple scales asymptotic techniques are to be invoked. See, e.g., [Schneider, 1978, Kevorkian and Cole, 1981] for textbook material on multi-scale asymptotics, and 4.2 below.

3.3 Physical considerations and scaling arguments

Here we provide first some physical interpretations for the scale-independent non-dimensional parameters introduced in the last section. Next we juxtapose the formal asymptotic *ansatz* proposed here with the physically motivated viewpoint of meteorological scaling analyses, and provide a “translation scheme” to mediate between the respective terminologies.

The universal scale-independent parameters

The first parameter, $\pi_1 = c_{\text{ref}}/(\Omega a)$ in (27) may be interpreted as a ratio of two propagation speeds. The quantity c_{ref} is of the order of the speed of sound. At the same time, it is proportional to the speed of long wavelength “barotropic”, i.e., vertically homogeneous, gravity waves. The product Ωa is the absolute velocity of points on the earth’s surface induced by its rotation. It is also the sun’s speed over ground near the equator. The estimate $c_{\text{ref}}/\Omega a < 1$ implies that, near the equator, the sun moves at supersonic speed relative to the earth’s surface. In other words: the main energy input into the atmosphere moves faster than the fastest gravity waves near the equator. (If not important, this occurs at least as an amusing observation.)

The second parameter, $\pi_2 = u_{\text{ref}}/c_{\text{ref}} =: M$, is the “Mach number”. Small Mach numbers indicate that changes of the fluid density due to compression by

inertial forces are small. At the same time, since c_{ref} has also been identified as the speed of barotropic gravity waves, π_2 is also the associated ‘‘Froude number’’.

The third parameter in (27) compares two characteristic length scales via the following interpretations

$$\pi_3 = \frac{\Omega c_{\text{ref}}}{g} = \frac{h_{\text{sc}}}{L_e}. \quad (35)$$

Here

$$h_{\text{sc}} = \frac{p_{\text{ref}}}{g\rho_{\text{ref}}} \sim 10 \text{ km} \quad (36)$$

is the *pressure scale height*, i.e., the characteristic vertical elevation over which the thermodynamic pressure of the atmosphere drops by a factor of order unity. In turn,

$$L_e = \frac{c_{\text{ref}}}{\Omega} \sim 3000 \text{ km} \quad (37)$$

is the *Obukhov radius* or *external Rossby deformation radius*. It is the horizontal distance that the fastest atmospheric gravity waves will travel before being influenced by the effects of earth rotation.

With these explanations, we obtain a new interpretation of our small expansion parameter ε . Using the distinguished limit from (28) we find

$$\frac{1}{\varepsilon} \sim \frac{\pi_2}{\pi_3} = \frac{g u_{\text{ref}}}{\Omega c_{\text{ref}}^2} = \frac{u_{\text{ref}}}{\Omega h_{\text{sc}}} =: \text{Ro}_{h_{\text{sc}}}, \quad (38)$$

where $\text{Ro}_{h_{\text{sc}}}$ is called the ‘‘Rossby number’’ based on the pressure scale height. Rossby numbers $\text{Ro}_\ell = u_{\text{ref}}/(\Omega\ell)$ formed with a reference length ℓ generally assess whether fluid motions at speed u_{ref} over distances of ℓ will or will not be affected by Coriolis effects, with small Rossby numbers indicating strong influences.

Scale-dependent non-dimensional parameters

Meteorological scale analysis obtains reduced model equations for specific flow phenomena by focusing on solutions of the full governing equations that are characterized by specific length and time scales. It is good common practice to quantify these scalings through appropriate non-dimensional characteristic numbers. In this section we demonstrate how various classical scaling relations of this type may be expressed within the present asymptotics-based framework.

As an example we choose the family of Rossby numbers with length ℓ as a free parameter, i.e.,

$$\text{Ro}_\ell = \frac{u_{\text{ref}}}{\Omega\ell}. \quad (39)$$

In the discussions of section 2 we have seen that

$$h_{\text{sc}} \ll L_1 \ll L_i \ll L_e, \quad (40)$$

and that each of these characteristic scales is associated with its own set of scale-dependent phenomena. In order to preserve this structure of scales and related physical effects in our asymptotic framework, we should preserve the ordering of

scales from (40) as $\varepsilon \rightarrow 0$. In fact, a quick check of equations (35) and (38) shows that the distinguished limits from (28) guarantee

$$L_1 \sim \frac{1}{\varepsilon} h_{sc}, \quad L_e \sim \frac{1}{\varepsilon^3} h_{sc}. \quad (41)$$

We can ensure in addition that $L_1 \ll L_i \ll L_e$, as required in (40), if

$$L_i \sim \frac{1}{\varepsilon^{\alpha+1}} h_{sc} \quad \text{as } \varepsilon \rightarrow 0 \quad \text{with} \quad 0 < \alpha < 2. \quad (42)$$

This, however, is not an immediate consequence of the basic order-of-magnitude estimates from Tables 2, 3. Instead, considering the definition of the internal Rossby radius of deformation,

$$L_i \sim \frac{N}{\Omega} h_{sc}, \quad (43)$$

equation (42) amounts to an asymptotic constraint for the Brunt-Väisälä-frequency N and, as a consequence, for the stratification of potential temperature, viz.

$$N = \sqrt{\frac{g}{\theta} \frac{\partial \theta}{\partial z}} \sim \frac{1}{\varepsilon^{\alpha+1}} \Omega. \quad (44)$$

This constraint should be observed in subsequent asymptotic expansions schemes. Fortunately, it is also compatible with evidence: Typical values for the Brunt-Väisälä-frequency in the troposphere are 0.01 s^{-1} , and 0.1 s^{-1} in the stratosphere, which leads to $\alpha \approx 1$ for the troposphere, and $\alpha \approx 2$ for the stratosphere, respectively, when $\varepsilon \sim 1/7$. However, up to now we have not found an intrinsic argument associated, e.g., with the radiation balance or with the transport of humidity, that would reveal the mechanisms responsible for establishing these orders of magnitude.

Given these qualifications, the Rossby numbers characterizing flow regimes associated with length scales h_{sc}, L_1, L_i, L_e , will have the following asymptotic scalings,

$$\begin{aligned} \text{Ro}_{h_{sc}} &= O(\varepsilon), \\ \text{Ro}_{L_1} &= O(1), \\ \text{Ro}_{L_i} &= O(\varepsilon^\alpha), \\ \text{Ro}_{L_e} &= O(\varepsilon^2). \end{aligned} \quad (45)$$

In the same fashion, one may relate ε to other scale-dependent dimensionless parameters that characterize particular flow regimes.

Coordinates for specific spatio-temporal scales

Here we explain how one can set up an asymptotic expansion in the present framework to study flows with a given characteristic length scale. As an example, we consider flows with characteristic scale L_i , the internal Rossby radius of deformation. The flow shall evolve on the characteristic advection time scale for this length,

$t_{\text{ref}} = L_i/u_{\text{ref}}$, and engulf the entire depth, h_{sc} , of the troposphere. In a meteorological scale analysis the appropriate non-dimensionalization of time and of the horizontal and vertical space coordinates would read

$$\tau = \frac{t' u_{\text{ref}}}{L_i}, \quad \boldsymbol{\xi} = \frac{\mathbf{x}'}{L_i}, \quad z = \frac{z'}{h_{\text{sc}}}, \quad (46)$$

where primes denote the original dimensional coordinates. The small non-dimensional parameter justifying the perturbation analysis would be the Rossby number based on the internal Rossby deformation radius L_i , i.e.,

$$\text{Ro}_{L_i} = \frac{u_{\text{ref}}}{\Omega L_i} \sim \frac{1}{10} \dots \frac{1}{5} \ll 1. \quad (47)$$

We would then seek solutions of the form

$$\mathbf{U} = \sum_i \text{Ro}_{L_i}^i \mathbf{U}^{(i)}(\tau, \boldsymbol{\xi}, z). \quad (48)$$

How would we go about analyzing the same situation within the present asymptotic framework? Suppose we chose the following non-dimensional coordinates in (33)

$$t = \frac{t' u_{\text{ref}}}{h_{\text{sc}}}, \quad \mathbf{x} = \frac{\mathbf{x}'}{h_{\text{sc}}}, \quad z = \frac{z'}{h_{\text{sc}}}. \quad (49)$$

From (42) we conclude that the dimensionless time and horizontal coordinates used in the scale analysis expansion (48) may be expressed as

$$\tau = \frac{t' u_{\text{ref}}}{h_{\text{sc}}} = \varepsilon^{\alpha+1} t, \quad \boldsymbol{\xi} = \frac{\mathbf{x}'}{L_i} = \varepsilon^{\alpha+1} \mathbf{x}, \quad (50)$$

while the vertical coordinate, z , remains unchanged. Furthermore, from (45) we have

$$\text{Ro}_{L_i} \sim \varepsilon^\alpha \quad (51)$$

so that (48) may be “translated” to

$$\mathbf{U}(t, \mathbf{x}, z; \varepsilon) = \sum_i (\varepsilon^\alpha)^i \mathbf{U}^{(i)}(\varepsilon^{\alpha+1} t, \varepsilon^{\alpha+1} \mathbf{x}, z). \quad (52)$$

Analogous “translation schemes” follow immediately when the relevant scales in the scale analysis approach can be expressed in terms of the length, time, and velocity scales considered here, i.e., in terms of $(h_{\text{sc}}, L_1, L_i, L_e, a)$, (N, Ω) , and $(u_{\text{ref}}, c_{\text{ref}})$.

There are situations, however, for which this condition is not satisfied. Consider, e.g., the flow over a hill of height $h \sim 500$ m, and horizontal extent $L \sim 3$ km. These scales are now imposed by orographical features rather than being directly related to the abovementioned basic scales. As a consequence, two new dimensionless parameters need to be accounted for. Without loss of generality we may choose the ratios

$$\frac{h}{h_{\text{sc}}}, \quad \text{and} \quad \frac{h}{L} \quad (53)$$

for this example. Both these parameters are small and may motivate perturbation analyses.

To cover such a case within the present scheme, one will have to decide upon the path to the origin in the space of parameters $\varepsilon, h/h_{sc}, L/h_{sc}$, as discussed in the context of Fig.4. For example, the concrete values for h and L given above would be compatible with

$$\frac{h}{h_{sc}} \sim 2 \cdot 10^{-1} = O(\varepsilon) \quad \text{and} \quad \frac{h}{L} \sim 0.6 \cdot 10^{-1} = O(\varepsilon). \quad (54)$$

With these distinguished limits, we can proceed via asymptotic expansions in ε based on the following set of coordinates for the perturbation functions

$$\mathbf{U}^{(i)}(t, \mathbf{x}, \frac{z}{\varepsilon}, z). \quad (55)$$

Here the coordinate z/ε will resolve flow structures comparable in height with the hill itself. The coordinates \mathbf{x}, z cover structures comparable with the horizontal extension of the hill as well as farfield effects in the vertical direction. A comprehensive discussion of flow effects induced by orography, surface roughness, and surface heat fluxes is work in progress with J.C.R. Hunt and A. Owinoh (see, e.g., [Hunt et al., 1988, Newley et al., 1991]).

3.4 “Pro’s and Con’s” of the present approach

Pro’s

1. The proposed approach directly relates any derived reduced models to the three-dimensional compressible flow equations in a transparent fashion.
2. There is a clear-cut mathematical route through each of the derivations. These have a common formal justification from the identification of a small number of universal, scale-independent small parameters and a related distinguished limit.
3. The approach prepares the ground for further studies of multiple scales interactions, see section 4.2.
4. Item 1 makes the present approach a natural starting point for developments of numerical methods for the compressible flow equations applicable to the various singular limit regimes of atmospheric flows, see section 4.3.
5. The identification of a nearly universal small parameter $\varepsilon \sim \frac{1}{7} \dots \frac{1}{6}$ provides an independent measure, besides empirical tests, for the regimes of validity of reduced model equations. Models derived for a characteristic length and time scales, L, T , (via scale analysis or via the present approach) loose credibility when the actual scales of a flow field considered cover a range that is comparable or larger than $\varepsilon L \dots L/\varepsilon, \varepsilon T \dots T/\varepsilon$. In such cases one must, in general, account for the possibility of scale interactions using multiple scales

techniques. We notice that $\varepsilon \sim 1/7 \dots 1/6$ is not extremely small in practice, so that the mentioned scale ranges are limited! On the other hand, reduced models *may* be applicable beyond the assessed ranges, but this requires additional empirical or theoretical justification.

Con's

1. The clear-cut mathematical route provided here may mislead newcomers into neglecting the physical and empirical bases for model reductions. It is relatively easy to come up with formal asymptotic derivations for all sorts of scales; the art is to identify, through careful physical considerations, those regimes that are of practical importance.
2. If we have managed to derive a particular reduced model via the present route, employing some particular distinguished limit and argument scalings. Then by no means does this guarantee that the adopted limit process is the only one leading to this model. In our example from Fig. 4 this could mean that the paths II and III, and any in between, yield the same result. Quantification of this degree of freedom requires additional analyses not discussed here.

4 Applications

Here we discuss three instructive applications in which the present approach proved useful. We will re-derive the well-known semi-geostrophic theory using multiple scales techniques in section 4.1, consider systematic multiple scales models from Majda and Klein [2003] in sectionssec:Tropics, and discuss recent developments of a “well-balanced” numerical method for nearly hydrostatic compressible flows in section 4.3.

4.1 Semi-geostrophic theory

Weather fronts are examples for atmospheric flow structures that feature anisotropic horizontal scalings. When viewed from above, one may think of a front as being a narrow band of activity centered about some smooth, large scale curve. All flow variables are expected to vary substantially over relatively short distances normal to the front, while they vary on scales comparable to the characteristic length of the curve’s geometry in the tangential direction.

An appropriate ansatz to capture this structural behavior in an asymptotic analysis, borrowed from WKB theories, geometrical optics/acoustics, or the theory of thin flames in combustion, could read

$$\mathbf{U}(t, \mathbf{x}, z; \varepsilon) = \sum_i \mathbf{U}^{(i)} \left(\varepsilon^2 t, \frac{\Phi(\varepsilon^2 \mathbf{x})}{\varepsilon}, \varepsilon^2 \mathbf{x}, z \right). \quad (56)$$

Here $\Phi(\cdot)$ is a scalar function, which by the scaling of its argument, $\varepsilon^2 \mathbf{x}$, in (56) will have a characteristic scale comparable to the internal Rossby deformation radius L_i (see the previous section). The scaled coordinate $\xi = \Phi/\varepsilon$ will then resolve

rapid variations of the solution that occur between levelsets $\Phi = \Phi_0 + O(\varepsilon)$. The front will thus be centered about the level set $\Phi(\varepsilon^2 \mathbf{x}) \equiv \Phi_0$ and have a characteristic thickness of order $\ell = O(\varepsilon L_i)$. According to (45), this is the characteristic length L_1 for which the Rossby number would be of order unity.

With the abbreviations

$$\tau = \varepsilon^2 t, \quad \xi = \frac{\Phi(\varepsilon^2 \mathbf{x})}{\varepsilon}, \quad \mathbf{X} = \varepsilon^2 \mathbf{x}, \quad (57)$$

the partial derivatives in the governing equations (1) become

$$\begin{aligned} \partial_t &= \varepsilon^2 \partial_\tau \\ \nabla &= \varepsilon \sigma \mathbf{n} \partial_\xi + \varepsilon^2 \nabla_{\mathbf{X}} + \mathbf{k} \partial_z. \end{aligned} \quad (58)$$

where $\sigma = |\nabla_{\mathbf{X}} \Phi|$ and $\mathbf{n} = \nabla_{\mathbf{X}} \Phi / |\nabla_{\mathbf{X}} \Phi|$. (We have left the complications of spherical geometry aside here, as they are not relevant to the main message of this section.)

A somewhat subtle issue in semi-geostrophic theory is the scaling of the velocity components. It is *assumed* that they scale in proportion with the characteristic length for their associated spatial direction. Thus one allows only the flow velocity tangential to the front to be of order u_{ref} , i.e., $\mathbf{v} \cdot \mathbf{t} = O(u_{\text{ref}})$, where $\mathbf{t}(\mathbf{X})$ is the tangential unit vector to a level set $\Phi = \text{const.}$. For the normal and vertical components this assumption implies $\mathbf{v} \cdot \mathbf{n} = O(\varepsilon u_{\text{ref}})$, and $\mathbf{v} \cdot \mathbf{k} = O(\varepsilon^2 u_{\text{ref}})$. Accordingly, the velocity field is represented as

$$\mathbf{v} = v^{(0)} \mathbf{t} + \varepsilon(v^{(1)} \mathbf{t} + u^{(1)} \mathbf{n}) + \varepsilon^2(v^{(2)} \mathbf{t} + u^{(2)} \mathbf{n} + w^{(2)} \mathbf{k}) + \dots \quad (59)$$

It is now straight-forward to insert the (56)–(59) into the governing equations from (1) and to collect the following leading order set of equations. Using the replacements

$$\begin{aligned} (\theta^{(4)}, p^{(4)}/\rho^{(0)}) &\rightarrow (\theta, \pi) \\ (u^{(1)}, v^{(0)}, w^{(2)}) &\rightarrow (u, v, w) \\ (S_\theta^{(6)}, S_v^{(2)}) &\rightarrow (S_\theta, S_v) \end{aligned} \quad (60)$$

we obtain the semi-geostrophic approximation (see [Pedlosky, 1987], section 8.4 for the case of an incompressible fluid)

$$\begin{aligned} -f v + \sigma \frac{\partial \pi}{\partial \xi} &= 0 \\ \frac{Dv}{D\tau} + f u^{(1)} + \frac{\partial \pi}{\partial \eta} &= S_v \\ \frac{\partial \pi}{\partial z} - \theta &= 0 \\ \frac{D\theta}{D\tau} &= S_\theta \\ \frac{\partial u}{\partial \xi} + \frac{\partial v}{\partial \eta} + \frac{1}{\rho_0} \frac{\partial}{\partial z} (\rho_0 w) &= 0, \end{aligned} \quad (61)$$

Here $\rho_0(z)$ is the background density stratification corresponding to a homentropic atmosphere,

$$\frac{D}{D\tau} = \frac{\partial}{\partial\tau} + v \frac{\partial}{\partial\eta} + u \sigma \frac{\partial}{\partial\xi} + w \frac{\partial}{\partial z}, \quad (62)$$

and

$$\frac{\partial}{\partial\eta} = \mathbf{t} \cdot \nabla_{\mathbf{X}}. \quad (63)$$

Lower order expansion functions, such as $\theta^{(2)}, \theta^{(3)}$ and $p^{(2)}, p^{(3)}$, which do not explicitly appear here, can be shown not to participate in the dynamics within a narrow front if the assumed time scaling is to be observed.

The semi-geostrophic equations are used in a range of contexts, including theories for the formation and structure of strong weather fronts. The key difference between these and the quasi-geostrophic equations discussed in section 2 is that only one of the horizontal velocity components, v , is in geostrophic balance. The velocity component normal to the front is, in contrast, the result of a balance between the Coriolis force, the pressure gradient, and the fluid particle acceleration along the front. The semi-geostrophic equations have, however, several attractive mathematical features, which are reviewed and extensively discussed, e.g., in [Hoskins, 1975, Cullen et al., 1991, Roulstone and Sewell, 1997, McIntyre and Roulstone, 2002]. One of these is the surprising fact that, by an ingenious nonlinear change of variables developed by Eliassen [1962], Hoskins and Bretherton [1972], and omission of *one* term they can be transformed into the quasi-geostrophic equations discussed in section 2.2.

Possible extensions Having re-derived another classical result within the present modelling framework, one may ask where to go next in the context of semi-geostrophic flows. Here are two possible lines of thought:

- We observe that analyses involving anisotropic scalings in the vicinity of a narrow front also occur, e.g., in the context of thin flame fronts in combustion. There, one is interested in (i) approximate equations governing the internal flame structure, and (ii) a flame propagation law that describes the flame's motion in space as time evolves. A slight modification of the asymptotic ansatz in (56) would allow us to transfer these ideas into the present context. One would introduce an explicitly time dependent level set function $\Phi(\varepsilon^2 t, \varepsilon^2 \mathbf{x})$ to define the front-resolving coordinate, and aim at extracting an evolution equation for this function by asymptotic matching with the surrounding flow.
- Another interesting option is to consider a faster time scale by allowing for an additional time coordinate εt in the asymptotic ansatz. This will lead to a multiple time variable expansion similar to [Embid and Majda, 1996, 1998, Majda and Embid, 1998, Babin et al., 2002], where the authors considered the averaged effects of fast gravity waves passing over quasi-geostrophical mean flows. It has been argued that strong weather fronts in fact undergo fast oscillations that affect their overall behavior non-trivially, and this problem could be investigated with the proposed modification of the analysis.

4.2 Synoptic-planetary interactions in the tropics

Here we summarize recent joint work with A.J. Majda addressing scale interactions in the tropics. A hierarchy of reduced model equations describing a range of possible flow regimes is derived by Majda and Klein [2003] using systematic multiple scales expansions. One particularly interesting regime involves interactions between the equatorial synoptic and the planetary scales. Here we review the flow regime and the key results of the analysis for this regime. For details the reader may consult the original reference.

Expansion scheme and scaling considerations

The multiple scales expansion scheme for this regime reads

$$\Phi(t, \mathbf{x}, z; \varepsilon) = \varepsilon^{\alpha(\Phi)} \sum_i \varepsilon^i \Phi^{(i)}(\varepsilon^{5/2}t, \varepsilon^{5/2}\mathbf{x}, \varepsilon^{7/2}x, z), \quad (64)$$

where $\alpha = 0$ for $\Phi \in \{p, \theta, \rho, \mathbf{u}\}$, and $\alpha = 1/2$ for $\Phi = w, S_\theta, S_v$. Here \mathbf{u}, w are the horizontal and vertical flow velocity components, respectively, and the coordinates $\mathbf{x} = (x, y)$ denote the zonal (along the equator) and meridional (north-south) horizontal coordinates. As we will see shortly, this scheme merges the single scale expansion for equatorial geostrophic motions,

$$\Phi(t, \mathbf{x}, z; \varepsilon) = \varepsilon^{\alpha(\Phi)} \sum_i \varepsilon^i \Phi^{(i)}(\varepsilon^{5/2}t, \varepsilon^{5/2}\mathbf{x}, z), \quad (65)$$

with a scheme that resolves planetary scale equatorial waves

$$\Phi(t, \mathbf{x}, z; \varepsilon) = \varepsilon^{\alpha(\Phi)} \sum_i \varepsilon^i \Phi^{(i)}(\varepsilon^{5/2}t, \varepsilon^{7/2}x, \varepsilon^{5/2}y, z). \quad (66)$$

The characteristic horizontal length scale accessed by the first scheme in (65) is the internal Rossby deformation radius for near-equatorial flows. To verify this, we reconsider the relation $L_i \sim Nh_{sc}/\Omega$ from (43). Near the equator, the earth rotation frequency Ω must be replaced with characteristic value of the vertical component $f = \mathbf{k} \cdot \boldsymbol{\Omega} = \Omega \sin(\phi)$ of the earth rotation vector, where ϕ is the longitude. In terms of the arclength in the meridional direction, y , we have $\phi = y/a$, where a is the earth's radius. Anticipating that $L_i \ll a$, which remains to be verified, we have $\sin(\phi) \sim L_i/a$, and $f \sim \beta L_i$, where $\beta = \Omega/a$. As a consequence,

$$L_i \sim \frac{N}{\beta L_i} h_{sc}, \quad \text{or} \quad \frac{L_i}{h_{sc}} \sim \sqrt{\frac{N}{\Omega} \frac{a}{h_{sc}}} \sim \varepsilon^{-5/2}. \quad (67)$$

The last estimate follows from equations (44) with $\alpha = 1$, and (41), which stated that $N/\Omega \sim \varepsilon^{-2}$ and $a/h_{sc} \sim \varepsilon^{-3}$. We verify that $L_i \ll a$, even though the difference is merely of order $\varepsilon^{1/2}$. Equation (67) shows that the scaling anticipated in (64) and (65) in fact accesses the internal Rossby deformation radius L_i .

The second expansion scheme in (66) accesses even larger (planetary) scales via the coordinate

$$X_P = \varepsilon^{7/2} x = \frac{x'}{L_P} \quad \text{with} \quad L_P = \varepsilon^{-7/2} h_{sc}. \quad (68)$$

Notice that this expansion assumes anisotropic scalings along and normal to the equator. This is compatible with theories of equatorial wave motions which reveal confinement of near-tropical dynamics between about -30° and 30° degrees latitude, see, e.g., [Gill, 1982, Majda, 2003].

The non-dimensional time coordinate in (64)–(66) may be re-written in two different ways:

$$\varepsilon^{5/2} t = \varepsilon^{5/2} \frac{t'}{h_{sc}/u_{ref}} = \frac{t'}{L_i/u_{ref}} = \frac{t'}{L_P/c_{i,ref}}, \quad (69)$$

where t' again denotes the dimensional time variable, and $c_{i,ref} \sim Nh_{sc}$ is the characteristic speed of internal gravity waves with vertical scale comparable to h_{sc} . This dual representation shows that, on the one hand, the chosen time coordinate resolves advection with the flow velocity u_{ref} over synoptic distances comparable to L_i . On the other hand, it also resolves internal gravity waves travelling at speeds $c_{i,ref}$ over planetary distances of the order L_P . As a consequence, the multiple scales expansion from (64) is suited to describe direct interactions of these very different phenomena on one and the same time scale.

Intra-Seasonal Planetary Equatorial Synoptic Dynamics (IPESD)

To simplify the notation, we will use the following replacements in the rest of this section:

$$\begin{aligned} (\theta^{(2)}, \theta^{(3)}, p^{(3)}/\rho^{(0)}, p^{(4)}/\rho^{(0)}) &\rightarrow (\Theta_2, \theta, \pi, \pi') \\ (\mathbf{u}^{(0)}, \mathbf{u}^{(1)}, w^{(2)}, w^{(3)}) &\rightarrow (\mathbf{u}, \mathbf{u}', w, w') \\ (S_\theta^{(4)}, S_\theta^{(5)}, \mathbf{S}_u^{(1)}, \mathbf{S}_u^{(2)}) &\rightarrow (S_\theta, S'_\theta, \mathbf{S}_u, \mathbf{S}'_u) \\ (\varepsilon^{5/2} t, \varepsilon^{5/2} \mathbf{x}, \varepsilon^{7/2} x) &\rightarrow (T_S, \mathbf{X}_S, X_P), \end{aligned} \quad (70)$$

where $\mathbf{X}_S = (X_S, Y_S)$.

Synoptic motions With the abbreviations from (70), the leading order set of equations describing motions on the smaller of the considered scales (which is still as large as 2000 km) reads

$$\begin{aligned} \partial_z \pi &= \theta \\ w \frac{d\Theta_2}{dz} &= S_\theta \\ -\beta y v + \partial_x \pi &= S_u \\ \beta y u + \partial_y \pi &= S_v \\ \partial_x(\rho_0 u) + \partial_y(\rho_0 v) + \partial_z(\rho_0 w) &= 0. \end{aligned} \quad (71)$$

These equations describe, in this sequence, hydrostatic balance in the vertical direction, the generation of vertical motions by heat sources forcing particles to move towards their individual levels of neutral buoyancy, horizontal geostrophic balance in the zonal (x) and meridional (y) directions, and mass conservation.

The equations in (71) may be considered as the three-dimensional version of the Matsuno-Webster-Gill type of models, [Matsuno, 1966, Webster, 1972, Gill, 1980, 1982], who derived models for steady forced synoptic scale motions near the equator in the context of the shallow water approximation (see also [Neelin, 1989, Majda and Klein, 2003]). Gill [1980, 1982] demonstrates that these equations reproduce typical quasi-steady large scale near-equatorial flow patterns when some physically reasonable closures for the source terms are assumed. His examples include qualitative models for the important ‘‘Hadley’’ and ‘‘Walker’’ circulations.

For given source terms S_θ, S_u, S_v the system in (71) is linear in u, v, w, π, θ . General solutions, in this case, are superpositions of particular and homogeneous solutions. One particular solution $u^p, v^p, w^p, \pi^p, \theta^p$ is determined by, [Majda and Klein, 2003],

$$w^p = \frac{S_\theta}{d\Theta_2/dz}, \quad v^p = \frac{1}{\beta} (S_{v,x} - S_{u,y}) + \frac{y}{\rho_0} \left(\frac{\rho_0 S_\theta}{d\Theta_2/dz} \right)_z, \quad (72)$$

$$\partial_x u^p = -\partial_y v^p - \frac{1}{\rho_0} \partial_z (\rho_0 w^p) \quad \text{with} \quad \beta y \overline{u^p} = \overline{S_v}, \quad (73)$$

$$\left. \begin{aligned} \partial_x \pi^p &= S_u - \beta y v^p \\ \partial_y \pi^p &= S_v + \beta y u^p \end{aligned} \right\} \quad \text{with} \quad \overline{\pi^p}(t, 0, z) \equiv 0, \quad (74)$$

$$\theta^p = \partial_z \pi^p. \quad (75)$$

Homogeneous solutions to (71) satisfy,

$$v = w \equiv 0, \quad (\theta, u, \pi) = (\Theta, U, P)(t, y, z), \quad (76)$$

where Θ, U, P are arbitrary except for the constraints

$$\partial_y P = -\beta y U, \quad \partial_z P = \Theta. \quad (77)$$

A few remarks regarding this synoptic scale model and the above particular solution are in order:

- With the present results we could extend Table 1 by adding the line

$\mathbf{U}^{(i)}(\varepsilon^{5/2}t, \varepsilon^{5/2}x, \varepsilon^{5/2}y, z)$ Forced quasi-steady equatorial synoptic motions

described by quasi-steady ‘‘Matsuno-Webster-Gill’’-models, [Matsuno, 1966, Webster, 1972, Gill, 1980, 1982].

- The equations incorporate a mechanism for the generation of large scale horizontal flow divergence from energy source terms. Heat addition through S_θ induces non-zero vertical velocities, which in turn drive horizontal flow divergences through the continuity of mass. In fact,

$$u_x + v_y = -\frac{1}{\rho_0} \left(\frac{\rho_0 S_\theta}{d\Theta_2/dz} \right)_z.$$

This mechanism is common to the family of “WTG” models, [Charney, 1963, Held and Hoskins, 1985, Browning et al., 2000, Bretherton and Sobel, 2001, A. Sobel et al., 2001, Majda and Klein, 2003], which are currently being used extensively in the context of tropical meteorology. These models are often derived on the basis of the assumption of **Weak horizontal Temperature Gradients**, and hence the acronym. Often, these models do not explicitly resolve all three space dimensions, but rather utilize Galerkin-type projections onto the dominant vertical flow modes to obtain reduced, effectively two-dimensional models, [Gill, 1980, Wang and Li, 1993, Neelin, 2000, Majda and Shefter, 2001]. This kind of further reduction could, of course, be applied here as well. We do not discuss this aspect here, as this step has no direct justification within the present asymptotic framework.

- There is a consistency condition on the spatial structure of the source terms. It is obtained by averaging the first equation in (74) with respect to x , and using the expression for v^p from (72),

$$\left(\frac{1}{y} \overline{S_u} \right)_y = \frac{\beta}{\rho_0} \left(\frac{\rho_0 \overline{S_\theta}}{d\Theta_2/dz} \right)_z. \quad (78)$$

When the source terms S_u, S_θ are considered to be given explicitly, then this is merely a constraint to be observed. If these source terms are, however, replaced with “parameterizations” of various net effects induced by small scale motions not resolved by the present model, the above constraint attains a quite different meaning. Generally, the source terms will then be functions of (π, θ, u, v, w) , and the consistency condition will introduce a functional relationship between these variables *that is entirely determined by the chosen parameterizations!* This corroborates the often-voiced warning that adequate parameterizations are at least as important for the success of a model as its fluid dynamical consistency.

From here on $u^p, v^p, w^p, \pi^p, \theta^p$ denote the particular solutions (72) to (75), and the source terms S_u, S_v, S_θ are assumed to satisfy (78).

Planetary waves As pointed out in conjunction with (76), the equation system for the synoptic scales determines solutions only up to a zonal (along the equator) shear flow. In the present context of a multiple scales expansion, this zonal shear flow may still not depend on x , but it may well depend on the planetary scale coordinate X_p , and multiple scales asymptotic techniques should allow us to derive evolution

equations for these large scale averaged mean motions. In fact, the following system is derived by Majda and Klein [2003],

$$\begin{aligned}
\overline{D_t^p} U + \partial_X P - \beta y \overline{v'} &= \overline{S'_u} - \overline{D_t^p u^p} \\
\overline{D_t^p} \Theta + \overline{w'} \frac{d\Theta_2}{dz} &= \overline{S'_\theta} - \overline{D_t^p \theta^p} \\
\beta y U + \partial_y P &= 0 \\
\partial_z P &= \Theta \\
\partial_X U + \partial_y \overline{v'} + \frac{1}{\rho_0} \partial_z (\rho_0 \overline{w'}) &= 0,
\end{aligned} \tag{79}$$

where

$$\begin{aligned}
D_t^p &= \partial_t + u^p \partial_x + v^p \partial_y + w^p \partial_z \\
\overline{D_t^p} &= \partial_t + \overline{v^p} \partial_y + \overline{w^p} \partial_z.
\end{aligned} \tag{80}$$

These equations are the three-dimensional analogue of the linear equatorial long wave equations, [Heckley and Gill, 1984], supplemented with the net large scale effects of the synoptic scale transport as represented by the terms, $\overline{D_t^p u^p}$, $\overline{D_t^p \theta^p}$, and with advection by the mean synoptic meridional velocity $\overline{v^p}$, see also [Majda and Klein, 2003]. Again, a few general remarks are in order:

- If we restrict here to very weak source terms, so that $S_u = S_v = S_\theta \equiv 0$ and, as a consequence, $(u^p, v^p, w^p, \theta^p, \pi^p) \equiv 0$, then the operators $D_t^p, \overline{D_t^p}$ reduce to the partial time derivative ∂_t , and the only source terms left in (79) are the perturbation source terms $\overline{S'_u}, \overline{S'_\theta}$.

The equations then describe the generation of linear equatorial long waves by weak momentum and energy sources, as in an inhomogeneous Heckley–Gill model, [Heckley and Gill, 1984]. We have thus successfully added another line to Table 1,

$$\mathbf{U}^{(i)}(\varepsilon^{5/2}t, \varepsilon^{7/2}x, \varepsilon^{5/2}y, z). \quad \text{Linear equatorial long wave motions}$$

- The equatorial synoptic scale may be estimated as $L_i \sim 2000$ km. Clearly, with $\varepsilon \sim 1/7$, a length scale of order L_i/ε must be expected to participate in the equatorial dynamics. Single scale expansions that do not acknowledge the presence of these asymptotically separated scales, will not be able to describe the scale interactions revealed in this section.

4.3 Balancing numerical methods for nearly hydrostatic motions

This section summarizes a quite different development that was motivated by our asymptotic considerations for atmospheric flows. Botta et al. [under revision; Preprint: PIK-Report No. 84, Potsdam Institute for Climate Impact Research (2002)] address a nagging numerical issue associated with the (asymptotically) dominant balance

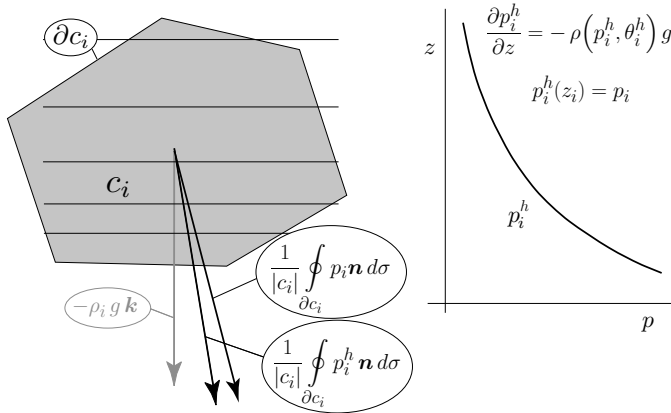


Figure 5. Archimedes' principle for the gravity source term.

between pressure forces and the gravitational acceleration in most realistic atmosphere flow regimes.

Consider the vertical component of the momentum balance in the dimensionless governing equations from (32), i.e.,

$$w_t + \mathbf{u} \cdot \nabla w + w w_z + \varepsilon \pi_3^* \mathbf{k} \cdot (\boldsymbol{\Omega} \times \mathbf{v}) + \frac{1}{\varepsilon^4} \left(\frac{1}{\rho} \frac{\partial p}{\partial z} + 1 \right) = S_w. \quad (81)$$

Suppose further that we had adopted a numerical discretization of all terms that is second order accurate in terms of the (vertical) space discretization parameter $h = \Delta z / h_{sc}$. Then the numerical truncation error induced by the two terms in (81) multiplied by $1/\varepsilon^4$ would read

$$\delta_{\text{num.}} = O\left(\frac{h^2}{\varepsilon^4}\right). \quad (82)$$

Current production runs with numerical weather forecasting or climate simulation codes use around 30 grid layers to resolve the vertical direction, so that $h \sim 1/30$. Our earlier estimates indicate that $\varepsilon \sim 1/7 \dots 1/6$, so that

$$\frac{h^2}{\varepsilon^4} = O(1) \quad (83)$$

under realistic conditions for up-to-date computational simulations of atmospheric flows. We conclude that the computed vertical accelerations will be highly inaccurate, unless special measures are taken to ensure that the limiting situation of hydrostatic balance is adequately captured by the numerical discretization.

Construction principle for a well-balanced scheme

Botta et al. [under revision; Preprint: PIK-Report No. 84, Potsdam Institute for Climate Impact Research (2002)] propose a quite generally applicable remedy for this

problem, and specifically describe an implementation in the context of conservative finite volume compressible flow solvers. The key ideas involved are as follows.

Archimedes' principle for the gravity source term: Figure 5 displays a general control volume that might serve as the i th grid cell c_i for our finite volume method. A straight-forward second order approximation of the gravity source term for such a volume would read

$$\int_{c_i} \rho \mathbf{k} d^2x = |c_i| \rho_i \mathbf{k} + O(\delta^2) \quad (84)$$

where ρ_i is the computed cell-averaged density and $|c_i|$ is the cell's volume, and $\delta = \text{diam}(c_i)$ is its characteristic diameter. In the context of conservative finite volume methods the integral of the pressure gradient over the volume is discretized as

$$\int_{c_i} \nabla p d^2x = \oint_{\partial c_i} p \mathbf{n} d\sigma = \sum_j A_{i,j} p_{i,j} \mathbf{n}_{i,j} + O(\delta^2) \quad (85)$$

where $A_{i,j}$, $p_{i,j}$, $\mathbf{n}_{i,j}$ are the length (area) of the j th section of the i th control volume's boundary, and approximations to the pressure and outward unit normal vector on that cell interface section. As indicated, these approximations are second order accurate in terms of δ . But this alone is insufficient to properly capture the hydrostatic limit, because the magnitude of the truncation errors is independent of whether the flow state is or is not close to hydrostatic.

To overcome this difficulty we observe that the vector $-\rho \mathbf{k}$ may be interpreted as the gradient of a virtual hydrostatic pressure distribution, i.e.,

$$\rho \mathbf{k} = -\nabla p^{\text{hy}}. \quad (86)$$

The gravity source term may then be rewritten as

$$\int_{c_i} \rho \mathbf{k} d^2x = - \oint_{\partial c_i} p^{\text{hy}} \mathbf{n} d\sigma = - \sum_j A_{i,j} p_{i,j}^{\text{hy}} \mathbf{n}_{i,j} + O(\delta^2). \quad (87)$$

As a consequence, the sum of the gravity source term and the pressure gradient is discretized as

$$\int_{c_i} (\nabla p + \rho \mathbf{k}) d^2x = \sum_j A_{i,j} (p_{i,j} - p_{i,j}^{\text{hy}}) \mathbf{n}_{i,j} + O(\delta^2 \|p - p_i^h\|), \quad (88)$$

where the $p_{i,j}^{\text{hy}} = p_i^{\text{hy}}(z_j)$ are values of a locally reconstructed virtual hydrostatic pressure distribution evaluated at the grid cell interface centers. (For the cell-wise construction of $p_i^{\text{hy}}(z)$ see below.) This modification will not change the approximation order of the scheme, which is still of second order for suitable formulations of the hydrostatic pressure distribution $p_i^h(z)$. Yet, we observe that the numerical approximate expression for the sum of the two terms now vanishes identically when the $p_{i,j}$ match the $p_{i,j}^{\text{hy}}$, i.e., when the pressure is hydrostatic in the sense of p_i^h .

Even if the approximate construction of p_i^h is inexact, so that $\|p - p_i^h\| \not\rightarrow 0$ as the hydrostatic limit is approached, the truncation error will be $O(\delta^2 \|p - p_i^h\|)$ instead of $O(\delta^2)$, and thus reduced as much as we manage to reproduce the local vertical balance.

Local hydrostatic reconstructions: The local hydrostatic pressure distributions $p_i^{\text{hy}}(z)$ obey

$$\frac{dp_i^h}{dz} = -\rho(p_i^h, \theta_i^h) g \quad (89)$$

with initial data

$$p_i^h(z_i) = p_i \quad (90)$$

where p_i is the pressure of the i th cell evaluated using the available cell averages of mass, momentum, and energy. The function $\theta_i^h(z)$ is a local approximate distribution of potential temperature as constructed from the cell-centered data via standard first or second order reconstruction formulae. In practice we have obtained very good results by using piecewise constant distributions $\theta_i^h(z) \equiv \theta_i$, while piecewise linear reconstructions yield further improvement.

Piecewise hydrostatic first order scheme: Standard first order finite volume schemes for hyperbolic conservation laws *without source terms* rely on an interpretation of the grid cell averages u_i of some conserved quantity u as providing cell-by-cell piecewise constant reconstructions

$$u^{\text{rec.}}(\mathbf{x}) = u_i \quad \text{for } \mathbf{x} \in c_i. \quad (91)$$

Second order schemes are then designed by improving these reconstructions, and to adopt piecewise linear or higher order polynomial distributions which are compatible with the grid cell averages at the cell centers. This approach satisfies the minimal requirement that spatially constant initial data, which constitute a stationary state for compatible boundary conditions, are also stationary in the discrete sense.

In the presence of, e.g., the gravity source term, this latter requirement is no longer satisfied, as stationary states feature non-trivial hydrostatic distributions of pressure and density. This incompatibility is avoided by adopting piecewise hydrostatic distributions as discussed in the last paragraph as the first order reference states. Higher order schemes are then constructed by piecewise polynomial reconstructions of *deviations* from these local hydrostatic states, [Botta et al., under revision; Preprint: PIK-Report No. 84, Potsdam Institute for Climate Impact Research (2002)].

Discussion and results

Properties of the well-balanced scheme The improved scheme just discussed has several desirable features.

- *Straight-forward implementation:*

The implementation of the balancing approach merely requires the re-formulation

of the gravity source term and application of discretization stencils to deviations from a hydrostatic state instead of deviations from piecewise constant distributions.

- *Flexibility w.r.t. the underlying base scheme:*

The design idea carries over to finite difference methods and finite element schemes. In fact, we have successfully implemented the approach in a test version of the local model “LM” of the Deutscher Wetterdienst (DWD), which uses finite difference discretizations.

- *Improved accuracy on a given grid:*

The scheme provides considerably improved accuracy *on a given grid* in comparison with the underlying non-balanced base scheme. Botta et al. [under revision; Preprint: PIK-Report No. 84, Potsdam Institute for Climate Impact Research (2002)] demonstrate that for some test cases one obtains the same accuracy with (i) the standard scheme using 80 vertical discretization layers and (ii) the well-balanced scheme using just 32 vertical layers. As compute time is a limiting factor in meteorological applications, this is of considerable interest in practice.

- *Robustness w.r.t. inessential details of a discretization:*

Non-balanced schemes are much more sensitive w.r.t. details of the numerical discretization scheme. For instance, we have found that the choice of a slope limiting function, used to avoid unphysical overshoots in the piecewise linear reconstructions of a second order scheme, will non-trivially affect the computational results. This is understood by comparing the reconstructions of the state variables at the left and right edges of a grid cell in the one-dimensional case for the standard and for the balanced scheme. With the standard approach, the value of some quantity u at, say, the right edge of the i th grid cell would be approximated as

$$u(x_{i+1/2}) \approx u_i + \frac{\Delta z}{2} \left(\frac{\partial u}{\partial z} \right)_i, \quad (92)$$

where

$$\left(\frac{\partial u}{\partial z} \right)_i = \text{Lim} \left(\frac{u_{i+1} - u_i}{\Delta z}, \frac{u_i - u_{i-1}}{\Delta z} \right). \quad (93)$$

Here $\text{Lim}(\cdot, \cdot)$ is some nonlinear limiting function that guarantees second order accuracy in the end, but avoids the generation of new extrema in the reconstructed distributions. Suppose now that u is near-hydrostatic, so that $u = u^{\text{hy}} + \delta u'$, where $\delta \ll 1$. Then the standard slope limiting procedure would essentially yield the limited slope of the hydrostatic distribution. As $\delta \rightarrow 0$ the result would depend on both the hydrostatic distribution and the choice of the limiting function. One will generally *not* obtain the exact hydrostatic states at the grid cell interfaces and, as a consequence, a hydrostatic state will generally not be a static state of the numerical method.

Consider now the reconstruction of the balanced scheme. Here we have

$$u(x_{i+1/2}) \approx u_i + (u^{\text{hy}}(x_{i+1/2}) - u_i) + \frac{\Delta z}{2} \left(\frac{\partial \delta u'}{\partial z} \right)_i, \quad (94)$$

where the slope limiting procedure is now applied only to deviations from the local hydrostatic distributions, i.e.,

$$\left(\frac{\partial \delta u'}{\partial z} \right)_i = \text{Lim} \left(\delta \frac{u'_{i+1} - u'_i}{\Delta z}, \delta \frac{u'_i - u'_{i-1}}{\Delta z} \right) \quad (95)$$

As $\delta \rightarrow 0$ this version will produce the exact hydrostatic state at $x_{i+1/2}$. Together with the Archmedes'-principle for the evaluation of the gravity source term we have a scheme that maintains any hydrostatic state exactly that is compatible with our local hydrostatic reconstruction based on piecewise constant or piecewise linear potential temperature distributions. For hydrostatic states not belonging to this class we still obtain considerable improvements as explained in the context of (88).

Sample results Unless the problem of unbalanced truncation errors explained above is addressed, numerical methods for flows under the influence of gravity will generate spurious motions under nearly hydrostatic conditions. This often becomes particularly prominent in the vicinity of steep orography as seen in Fig. 6.

There are classes of vertical distributions of potential temperature (entropy) for which the well-balanced scheme described above is able to reproduce the steady state up to machine accuracy by construction. These involve piecewise constant and piecewise linear distributions, in particular. For more general distributions, the truncation error is still reduced considerably as explained in the context of equation (88) above. An important example is an ‘‘inversion situation’’, for which the vertical gradient of potential temperature changes abruptly between several limited vertical layers of air. Figure 7 shows the time evolution of vertical velocity for a test case involving hydrostatic initial conditions in the vicinity of a 2 km high ‘‘mountain’’ and with the following vertical distributions of the Brunt-Väisälä-frequency.

$$N = N_i \quad \text{for} \quad z_i \leq z < z_{i+1} \quad (i \in \{0, 1, 2\}) \quad (96)$$

where

$$z_0 = 0 \text{ m}, \quad z_1 = 750 \text{ m}, \quad z_2 = 1\,250 \text{ m}, \quad z_3 = 8\,000 \text{ m}. \quad (97)$$

Here z_3 indicates the top of the computational domain, where the initial data are imposed as external states in the computation of boundary fluxes. On these boundaries, the fluxes are obtained by approximately solving Riemann problems. These problems are defined in terms of the states reconstructed inside the computational domain and the imposed external states. This formulation is also used at the lateral boundaries. (See the legends for values of N .) The graph shows that the maximum (spurious) vertical velocities for all cases considered do not exceed 0.1 m/s, and remain as small as a few centimeters per second in general. This is in sharp contrast with the situation displayed in Fig. 6, obtained with the standard scheme, where

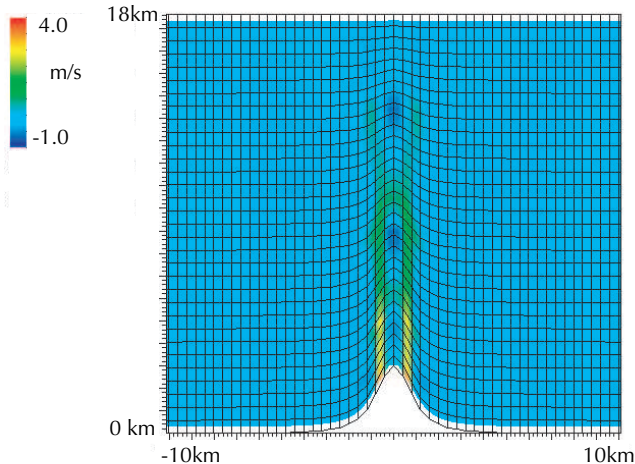


Figure 6. *Spurious vertical winds in the vicinity of steep orography generated by an unbalanced conservative finite volume method, [Botta et al., under revision; Preprint: PIK-Report No. 84, Potsdam Institute for Climate Impact Research (2002)]. An 18 km high layer of air at rest is placed near a 3 km high “mountain”. Vertical winds of up to 4 m/s are observed within about 60 min physical time on a computational grid with 32×128 grid points. The graph shows a color-plot of vertical velocity in a $-10 \dots 10$ km vicinity of the orographical feature, involving about 50 gridpoints in the horizontal direction.*

vertical velocities reached levels of 4 m/s, a level that is entirely unacceptable for meteorological applications. For details of this test case, the reader is referred to the original reference.

With the well-balancing approach in place, the finite volume compressible flow solver is now competitive in terms of accuracy with other well-established numerical techniques used in numerical weather forecasting. Its advantage is that it implements conservation of mass and energy up to machine accuracy, and momentum conservation in cases where the momentum source terms have a divergence form representation. Results for a challenging test case involving lee wave generation over non-trivial terrain from Schär et al. [2002] are shown in Fig. 8.

The test case involves dry air flow past the “wavy” topography

$$z_b(x) = h \exp\left(-\frac{x^2}{a^2}\right) \cos^2\left(\frac{\pi x}{\lambda}\right) \quad (98)$$

where $h = 250$ m, $a = 5$ km, and $\lambda = 4$ km. The Brunt-Väisälä-frequency is assumed constant at $N = 0.01 \text{ s}^{-1}$, and the bottom pressure and temperature are set to $p_0 = 10^5 \text{ kg/ms}^2$ and $T_0 = 273, 16 \text{ K}$, respectively. The horizontal flow velocity imposed at the upstream (left) entrance to the domain is 10 m/s for $0 \leq z \leq 10.395$ km, and decreases linearly to zero from there to the top of the domain at 19.5 km. The vertical velocity is set to zero throughout the domain initially. The boundary

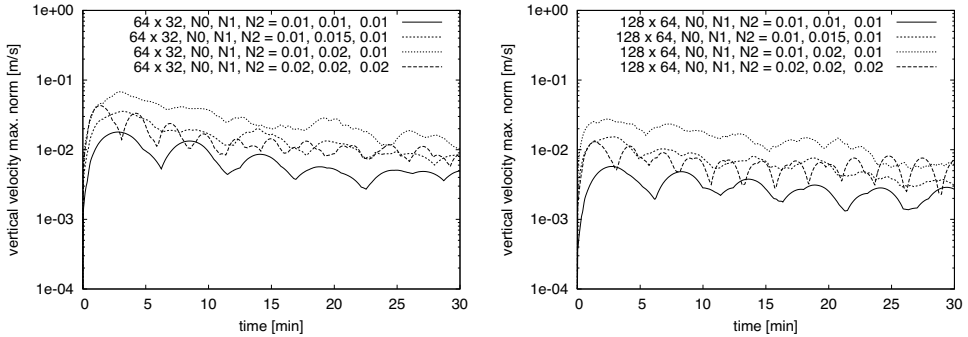


Figure 7. *Remaining spurious motions for an inversion situation with piecewise constant vertical distributions of the Brunt-Väisälä-frequency N (see (44)).*

condition formulation is the same as that explained above in the context of the static cases without mean flow.

Figure 8 shows contours of the vertical velocity after the solution has reached near steady state conditions. These results are consistent with those obtained by Schär et al. [2002] as a result of linear perturbation theory. At the same time they are comparable in terms of quality with their simulations using the canadian MC2-model, [Benoit et al., 1997], and a newly proposed computational grid structure that drastically reduces grid distortions away from the bottom topography. Our results have been computed using the well-balanced conservative finite volume scheme on a standard terrain-following grid without such modifications, albeit with a 20 % higher spatial resolution. For further details the reader is referred once more to the original references.

5 Conclusions

The present paper proposes a systematic approach, based on techniques of multiple scales asymptotics, for structuring the vast variety of reduced model equations of theoretical meteorology. The bottom line of the approach has been summarized focusing on the fluid mechanics of atmospheric motions. “Diabatics”, i.e. energetic processes, boundary layer problems, and many other meteorological processes of interest are not addressed here, due to both a lack of space and the fact that further work is still needed in this direction.

The concrete applications of the technique may have convinced the reader that it gives rise to interesting extensions of existing theories, that it leads to novel multi-scale models, and that it is quite useful also in the analysis of numerical methods.

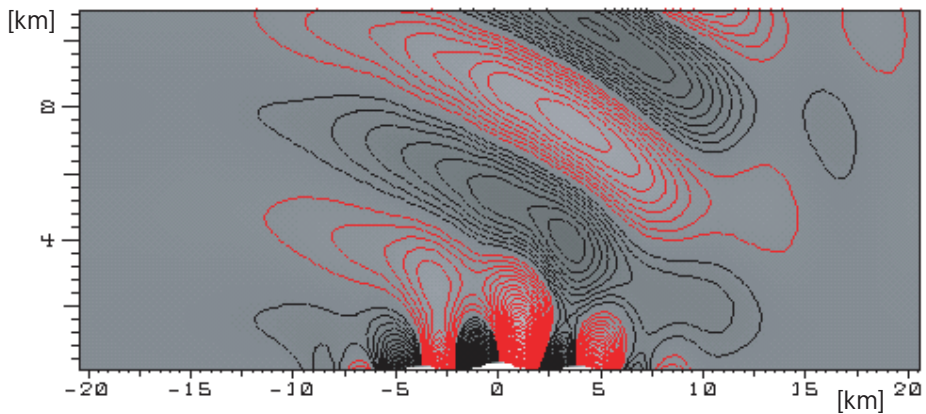


Figure 8. *Steady state lee waves over complex terrain in a test case taken from Schär et al. [2002] represented by contours of the vertical velocity. Computations are based on the present well-balanced conservative finite volume scheme, and a grid resolution of 800×128 nearly equally spaced grid cells for the discretization of the computational domain covering $19.5 \text{ km} \times 200 \text{ km}$. A single “bump” is thus resolved by about 10 grid cells. Only a $9.5 \text{ km} \times 40 \text{ km}$ near-topography subdomain, resolved by about 160×64 grid cells, is shown.*

Bibliography

- A. A. Sobel, J. Nilsson, and L. Polvani. The weak temperature gradient approximation and balanced tropical moisture waves. *Journal of Atmosphere Sciences*, 58:3650–3665, 2001.
- U. Achatz and G. Branstator. A two-layer model with empirical linear corrections and reduced order for studies of internal climate variability. *Journal of Atmosphere Sciences*, 56:3140–3160, 1999.
- A. Babin, A. Maholov, and B. Nicolaenko. Fast singular limits of stably stratified 3d euler and navier-stokes equations and ageostrophic wave fronts. In J. Norbury and I. Roulstone, editors, *Large-Scale Atmosphere-Ocean Dynamics 1: Analytical Methods and Numerical Models*, pages 126–201. Cambridge University Press, 2002.
- R. Benoit, M. Desgagne, P. Pellerin, S. Pellerin, Y. Chartier, and S. Desjardin. The canadian mc2: A semi-lagrangian, semi-implicit wide-band atmospheric model suited for finescale process studies and simulation. *Monthly Weather Review*, 125:2382–2415, 1997.
- N. Botta, R. Klein, and A. Almgren. Asymptotic analysis of a dry atmosphere. In *ENUMATH, Jyväskylä, Finland*, 1999.
- N. Botta, R. Klein, S. Langenberg, and S. Lützenkirchen. Well-balanced finite volume methods for near-hydrostatic flows. *Journal of Computational Physics*, under revision; Preprint: PIK-Report No. 84, Potsdam Institute for Climate Impact Research (2002).
- C. Bretherton and A. Sobel. The gill model and the weak temperature gradient (wtg) approximation. *Journal of Atmosphere Sciences*, 60:451–460, 2001.
- G. Browning, H. O. Kreiss, and W. H. Schubert. The role of gravity waves in slowly varying in time tropospheric motions near the equator. *Journal of Atmosphere Sciences*, 57:4008–4019, 2000.
- E. Buckingham. Model experiments and the forms of empirical equations. *Transactions of the American Society of Mechanical Engineers*, 37:263–296, 1915.

- P. Cargo and A.Y. Le Roux. Un schéma équilibre adapté au modèle d'atmosphère avec termes de gravité. *C. R. Acad. Sci. Paris*, 318:73–76, 1994.
- J. G. Charney. A note on large-scale motions in the tropics. *Journal of Atmosphere Sciences*, 20:607–609, 1963.
- A. Conaty, J. Jusem, L. Takacs, D. Keyser, and R. Atlas. The structure and evolution of extratropical cyclones, fronts, jet streams, and the tropopause in the geos general circulation model. *Bull. Amer. Meteorol. Soc.*, 82:1853–1867, 2001.
- M. J. P. Cullen, J. Norbury, and R.J. Purser. Generalized lagrangian solutions for atmospheric and oceanic flows. *SIAM J. Appl. Math.*, 51:20–31, 1991.
- D. R. Durran. Improving the anelastic approximation. *Journal of Atmosphere Sciences*, 46:1453–1461, 1989.
- D. G. Ebin. Motion of slightly compressible fluids in a bounded domain. *Comm. Pure Appl. Math.*, 35:451–485, 1982.
- A. Eliassen. On the vertical circulation in frontal zones. *Geophys. Publ.*, 24:147–160, 1962.
- P. Embid and A. J. Majda. Averaging over fast gravity waves for geophysical flows with arbitrary potential vorticity. *Comm. Partial Diff. Eqns.*, 21:619–658, 1996.
- P. Embid and A. J. Majda. Low froude number limiting dynamics for stably stratified flow with small or finite rossby numbers. *Geophys. Astrophys. Fluid Dynamics*, 87:1–50, 1998.
- A. E. Gill. Some simple solutions for heat-induced tropical circulation. *Quart. J. Roy. Met. Soc.*, 87:447–462, 1980.
- A. E. Gill. *Atmosphere-Ocean Dynamics*, volume 30 of *Intl. Geophysics Series*. Academic Press, San Diego, 1982.
- W. A. Heckley and A. E. Gill. Some simple analytical solutions to the problem of forced equatorial long waves. *Quart. J. Roy. Met. Soc.*, 110:203–217, 1984.
- I. M. Held and B. J. Hoskins. Large-scale eddies and the general circulation of the troposphere. *Advances in Geophysics*, 28:3–31, 1985.
- B. J. Hoskins. The geostrophic momentum approximation and the semi-geostrophic equations. *Journal of Atmosphere Sciences*, 32:233–242, 1975.
- B. J. Hoskins and F. P. Bretherton. Atmospheric frontogenesis models: mathematical formulation and solution. *Journal of Atmosphere Sciences*, 29:11–37, 1972.
- J.C.R. Hunt, K.J. Richards, and P.W.M. Brighton. Stably stratified shear flow over low hills. *Q.J.R. Met. Soc.*, 114:859–886, 1988.
- J. Kevorkian and J. D. Cole. *Perturbation methods in Applied Mathematics*, volume 34 of *Applied Mathematics Sciences*. Springer-Verlag, New York, 1981.

- S. Klainerman and A. J. Majda. Compressible and incompressible fluids. *Comm. Pure Appl. Math.*, 35:629–656, 1982.
- R. Klein. Asymptotic analyses for atmospheric flows and the construction of asymptotically adaptive numerical methods. *Zeitschr. Angew. Math. Mech.*, 80:765–777, 2000.
- A. Majda and R. Klein. Systematic multi-scale models for the tropics. *Journal of Atmosphere Sciences*, 60:393–408, 2003.
- A. Majda and J. Sethian. The derivation and numerical solution of the equations for zero mach number combustion. *Combustion Science and Technology*, 42:185–205, 1985.
- A. Majda and M. Shefter. Models for stratiform instability and convectively coupled waves. *Journal of Atmosphere Sciences*, 58:1567–1584, 2001.
- A. Majda, I. Timofeyev, and E. Vanden-Eijnden. Systematic strategies for stochastic mode reduction in climate. *J. Atmos. Sci.*, 60:1705–1722, 2003.
- A. J. Majda. *Introduction to PDE's and Waves for the Atmosphere and Ocean*. Lecture Notes from Courant Institute 2000-2001. American Mathematical Society, 2003.
- A. J. Majda and P. Embid. Averaging over fast gravity waves for geophysical flows with unbalanced initial data. *Theoretical and Computational Fluid Dynamics*, 11:155–169, 1998.
- T. Matsuno. Quasi-geostrophic motions in the equatorial area. *J. Met. Soc. Jap.*, 44:25–43, 1966.
- M. E. McIntyre and I. Roulstone. Are there higher-accuracy analogues of semi-geostrophic theory? In *Large-scale Atmosphere-Ocean Dynamics II: Geometric Methods and Models*. Cambridge University Press, 2002.
- J. D. Neelin. On the integration of the gill model. *Journal of Atmosphere Sciences*, 46:2466–2468, 1989.
- J. D. Neelin. A quasi-equilibrium tropical circulation model–formulation. *Journal of Atmosphere Sciences*, 57:1741–1766, 2000.
- T.M.J. Newley, H.J. Pearson, and J.C.R. Hunt. Stably stratified rotating flow through a group of obstacles. *Geophys. Astrophys. Fluid Dynamics*, 58:147–171, 1991.
- Y. Ogura and N. A. Phillips. Scale analysis of deep moist convection and some related numerical calculations. *Journal of Atmosphere Science*, 19:173–179, 1962.
- J. Pedlosky, editor. *Geophysical Fluid Dynamics*. Springer, 2 edition, 1987.

- V. Petoukhov, A. Ganopolski, V. Brovkin, M. Claussen, A. Eliseev, C. Kubatzki, and S. Rahmstorf. Climber-2: A climate system model of intermediate complexity. part i: Model description and performance for the present climate. *Climate Dynamics*, 16:1–17, 2000.
- S. Rahmstorf and A. Ganopolski. Long-term global warming scenarios computed with an efficient coupled climate model. *Climatic Change*, 43:353–367, 1999.
- I. Roulstone and M.J. Sewell. The mathematical structure of theories of semi-geostrophic type. *Phil. Trans. Roy. Soc. London, A* 355:2489–2517, 1997.
- B. Saltzman. A survey of statistical-dynamical models of the terrestrial climate. *Adv. Geophysics*, 20:183–304, 1978.
- C. Schär, D. Leuenberger, O. Fuhrer, D. Lüthi, and C. Girard. A new terrain-following vertical coordinate formulation for atmospheric prediction models. *Monthly Weather Review*, 130:2459–2480, 2002.
- W. Schneider, editor. *Mathematische Methoden in der Strömungsmechanik*. Vieweg, 1978.
- S. Schochet. Fast singular limits of hyperbolic pdes. *Journal of Differential Equations*, 114:476–512, 1994.
- W. Schröder, editor. *Ertel's potential vorticity. (Ertel's collected papers Vol. III)*. Interdivisional Commission on History of IAGA / History Commission of the German Geophysical Society, 1997.
- P. Stone and M.-S. Yao. Development of a two-dimensional zonally averaged statistical-dynamical model. part iii: The parameterization of the eddy fluxes of heat and moisture. *J. Climate*, 3:726–740, 1990.
- B. Wang and T. Li. A simple tropical atmosphere model of relevance to short-term climate variations. *Journal of Atmosphere Sciences*, 50:260–284, 1993.
- P. J. Webster. Response of the tropical atmosphere to local steady forcing. *Monthly Weather Review*, 100:518–541, 1972.
- R. K. Zeytounian, editor. *Meteorological Fluid Dynamics*. Lecture Notes in Physics, m5. Springer, 1991.